Bubble columns for condensation at high concentrations of noncondensable gas: Heat-transfer model and experiments

Citation: Narayan, G. Prakash, Mostafa H. Sharqawy, Steven Lam, Sarit K. Das, and John H. Lienhard. "Bubble Columns for Condensation at High Concentrations of Noncondensable Gas: Heat-Transfer Model and Experiments." AIChE Journal 59, no. 5 (May 2013): 1780–1790.

As Published: http://dx.doi.org/10.1002/aic.13944

Publisher: Wiley Blackwell

Persistent URL: http://hdl.handle.net/1721.1/86334

Version: Author's final manuscript: final author's manuscript post peer review, without publisher's formatting or copy editing

AIChE Journal
DOI 10.1002/aic.13944

Bubble columns for condensation at high concentrations of non-condensable gas: heat transfer model and experiments

G. Prakash Narayan[a], Mostafa H. Sharqawy[b], Steven Lam[a], Sarit K. Das[c], John H. Lienhard V[a,*]

[a] *Department of Mechanical Engineering, Massachusetts Institute of Technology, Cambridge, USA.*
[b] *Department of Mechanical Engineering, King Fahd University of Petroleum and Minerals, Dhahran, Saudi Arabia.*
[c] *Department of Mechanical Engineering, Indian Institute of Technology - Madras, Chennai, India.*

Abstract

Carrier gas based thermodynamic cycles are common in water desalination applications. These cycles often require condensation of water vapor out of the carrier gas stream. Since the carrier gas is most likely a non-condensable gas present in very high concentrations (60-95%), a large additional resistance to heat transfer is present. We propose to reduce the aforementioned thermal resistance by condensing the vapor-gas mixture in a column of cold liquid rather than on a cold surface by using a bubble column heat exchanger. A theoretical predictive model for estimating the heat transfer rates and new experimental data to validate this model are described. The model is purely physics based without the need for any adjustable parameters, and it is shown to predict heat rates within 0% to -20% of the experimental values. The experiments demonstrate that heat transfer rates in the proposed device are up to an order magnitude higher than those achieved in existing state-of-the-art dehumidifiers.

Keywords: condensation, bubble column, non-condensable gas, thermal resistance model, dehumidification, moist air, carrier gas

*Corresponding author
Email address: lienhard@mit.edu (John H. Lienhard V)

Received: Mar 06, 2012; Revised: Aug 30, 2012; Accepted: Sep 10, 2012

Nomenclature

Notation

a_s	specific interfacial area of the bubble column (m^2/m^3)
c	flexible constant used by Deckwer[1] (-)
c_p	specific heat capacity at constant pressure (J/kg·K)
$c_{p,g}$	average specific heat capacity at constant pressure of the vapor-air mixture (J/kg·K)
D_{AB}	diffusion coefficient (m^2/s)
D_b	bubble diameter (m)
d_o	sparger hole diameter (m)
g	gravitational accelaration (m/s^2)
H	liquid height in the column (m)
h	heat transfer coefficient ($W/m^2 \cdot K$)
h_{air}	specific enthalpy of air-vapor mixture (J/kg dry air)
h_{fg}	specific enthalpy of vaporization (J/kg)
h_t	heat transfer coefficient for the sensible heat exchanged between bubble and liquid column ($W/m^2 \cdot K$)
j	mass flux ($kg/m^2 \cdot s$)
k	thermal conductivity (W/m·K)
k_l	mass transfer coefficient (m/s)
l	characteristic length (m)
l_{int}	integral length for turbulence (m)
$\dot{m}$	mass flow rate (kg/s)
n	exponent (-)
q	heat flux (W/m^2)
q_{lt}	heat flux due to condensation of vapor from the bubble in the liquid column (W/m^2)
$q_{lt,impact}$	heat flux due to direct condensation of vapor from the bubble on the coil surface (W/m^2)
$q_{sensible}$	heat flux due to the sensible heat exchange between bubble and liquid column (W/m^2)
R	Thermal resistance ($K \cdot m^2/W$)
R_{bc}	Thermal resistance between the liquid column and the coil surface ($K \cdot m^2/W$)
R_{coil}	Thermal resistance due to coolant flow inside the coil ($K \cdot m^2/W$)
R_{bc}	Thermal resistance between the liquid column and the coil surface ($K \cdot m^2/W$)
R_m	Mass transfer resistance ($s \cdot m^2/kg$)

$R_{sensible}$	Thermal resistance for the sensible heat exchange between bubble and liquid column (K·m^2/W)
t	surface renewal time (s)
t_f	average residence time of the bubble in the liquid (s)
T	temperature (°C)
T_{air}	local energy-averaged temperature of the air-vapor bubble (°C)
T_{coil}	local temperature of the coil surface (°C)
T_{column}	local energy-averaged temperature of the liquid in the column (°C)
$T_{coolant}$	local energy-averaged temperature of the coolant in the coil (°C)
u	velocity in the x direction (m/s)
V	velocity (m/s)
V_b	bubble velocity (m/s)
V_c	circulation velocity (m/s)
V_g	superficial velocity (m/s)
V_r	radial velocity in the liquid column (m/s)
vol	volume of the bubble column (m^3)

Greek letters

α	thermal diffusivity (m^2/s)
∂	operator for partial derivative (-)
ϵ	volumetric gas holdup (-)
ε	turbulent energy dissipation rate per unit mass (m^2/s^3)
θ	log mean temperature difference (°C)
ν	kinematic viscosity (m^2/s)
ρ	density (kg/m^3)
σ	surface tension (N/m)
ω	absolute humidity (kg water vapor per kg dry carrier gas)
χ	mole fraction (mol/mol)

Subscripts

da	dry air
l	liquid
g	gas
in	entering
out	leaving
sat	saturated state

Non-dimensional Numbers

Fr	Froude Number, $V_g^2/(g \cdot D_b)$
Le	Lewis Number, α/D_{AB}
$\mathrm{Le_f}$	Lewis Factor, $h_t/(\rho c_{p,g} k_l)$
Pr	Prandl Number, ν/α
Re	Reynolds Number, $(V_g \cdot D_b)/\nu$
St	Stanton Number, $h/(\rho c_p V_g)$

Introduction

When a non-condensable gas is present, the thermal resistance to condensation of vapor on a cold surface is much higher than in a pure vapor environment. This is, primarily, because of the diffusion resistance to transport of vapor through the mixture of non-condensable gas and vapor. Several researchers have previously studied and reported this effect[2–10]. There is a general consensus that, when even a few mole percent of non-condensable gas is present in the condensing fluid, the deterioration in the heat transfer rates could be up to an order of magnitude[11–16]. From experimental reports in literature it can be observed that the amount of deterioration in heat transfer is a very strong (almost quadratic) function of the mole fraction of non-condensable gas present in the condensing vapor. For this reason, a deaerator is usually used in power plants to prevent the accumulation of non-condensable gas in the steam condenser. However in other applications, including water desalination, the presence of air in steam condensation is not always avoidable.

In desalination systems using air as a carrier gas, a large percentage of air (60-95% by mass) is present by default in the condensing stream. As a consequence it has been found that, in these systems, the heat exchanger used for condensation of water out of an air-vapor mixture (otherwise known as dehumidifier) has very low heat transfer coefficients (as low as 1 $W/m^2 \cdot K$ in some cases[17,18]). In this paper, we propose to improve the heat transfer rate by condensing the vapor-gas mixture in a column of cold liquid rather than on a cold surface by using a bubble column heat (and mass) exchanger.

Bubble columns are extensively used as multiphase reactors in process, biochemical and metallurgical applications[19]. They are used especially in chemical processes involving reactions which have a very high heat release rate associated with them (such as the Fischer-Tropsch process used in the manufacture of synthetic fuels)[20,21]. We propose to apply this device for condensation of the air-vapor mixture with a large percentage of air present in it. Figure 1 illustrates the proposed device schematically. In this device, moist air is sparged through a porous plate (or any other type of sparger[22]) to form bubbles in a pool of cold

liquid. The upward motion of the air bubbles causes a wake to be formed underneath the bubble which entrains liquid from the pool, setting up a strong circulation current in the liquid pool[23]. Heat and mass are transferred from the air bubble to the liquid in the pool in a direct contact transport process. At steady state, the liquid, in turn, loses the energy it has gained to the coolant circulating through a coil placed in the pool for the purpose of holding the liquid pool at a steady temperature.

[Figure 1 about here.]

Predictive model for combined heat and mass transfer

In this section, we develop a thermal resistance model for the condensation of water from an air-vapor mixture in a bubble column heat exchanger. Figure 2 illustrates a local thermal resistance network describing the heat and mass transfer processes in the bubble column condenser. To draw this network, we define local energy-averaged 'bulk' temperatures for the condensing mixture, the liquid in the pool, and the coolant and also approximate the heat transfer to be locally one-dimensional.

[Figure 2 about here.]

The four temperature nodes in the network are: (1) the average local temperature of the air-vapor mixture in the bubbles (T_{air}), (2) the average temperature of the liquid in the pool (T_{column}), (3) the local temperature of the coil surface (T_{coil}), and (4) the average local temperature of the coolant inside the coil ($T_{coolant}$). Between T_{air} and T_{column} there is direct contact heat and mass transfer. The heat transfer is via a thermal resistance represented by $R_{sensible}$ and the mass transfer is represented as a (latent) heat source ($q_{lt} = j \cdot h_{fg}$). The thermal resistance due to the coil wall itself will be very small and has been neglected. This is especially true in the cases considered in this paper since copper tubing is used. In cases where stainless steel or a lower thermal conductivity metal is used, this resistance might not be negligible. Between the coil surface and the bubble there could be direct contact

heat exchange and associated condensation of vapor on the coil surface. The heat transfer is via a heat transfer resistance R_{impact} and the mass transfer are represented by the heat source $q_{lt,impact}$. Several researchers[1,20,21,24,25] have previously studied the thermal resistance between the pool of liquid and the immersed surface in a bubble column reactor. In the current paper, this resistance is represented as R_{bc} between T_{coil} and T_{column}. Finally, there is a convective resistance inside the coil for the coolant flow represented by R_{coil}.

In order to simplify the circuit, the direct impact of the bubble on the coil surface is approximated to have negligible effect on the heat and mass transfer (i.e. R_{impact} and $q_{\text{lt,impact}}$ are neglected). The experiments were designed and carried out such that this approximation was satisfied (see section c) and the effect of direct impact was dealt with in a separate set of experiments (see section c). Each of the remaining resistances depicted above will be modeled using reasonable simplifying assumptions in the following paragraphs.

Thermal resistance between the liquid in the column and the coil surface

In bubble column reactors used in the chemical industry, proper design of the heat transfer surfaces is vital to maintain catalytic activity, reaction integrity and product quality since the reactions typically involve very high heat release rates because of their highly exothermic or endothermic nature. In these scenarios, the temperature of the liquid in the column is of utmost importance. Hence, several studies have been conducted over the last five decades on modeling and measuring the heat transfer coefficients between the liquid and the heat transfer surface.

In a pioneering effort, Konsetov[24] proposed a semi-analytical model based on the assumption that heat rates are determined by isotropic turbulent fluctuations in the liquid. He approximated the characteristic dimension for heat transfer from the liquid to the coil to be the coil diameter and used the Kutateladze model[26] for determining the gas holdup. Konsetov used a flexible constant to fit the data from the model to experimental data in literature. This correlation, however, has not been widely used for bubble column reactor design.

Kast[25] developed a model by considering that a fluid element in front of the rising bubble receives radial momentum and moves toward the wall. This was postulated to break up the boundary layer at the wall. The author proposed that below the bubble, liquid is sucked in at a radial velocity V_r and that this results in a capacitive heat transport given by $V_r \cdot \rho \cdot c_p$. He further observed that V_r is propotional to the superficial gas velocity V_g and defined Stanton number as $St = \frac{h}{\rho_l \cdot c_{p,l} \cdot V_g}$. Based on intuitive reasoning Kast proposed the following correlation.

$$St = f(ReFrPr)^n \tag{1}$$

Deckwer[1] used the Kolmogorov theory of isotropic turbulence[27] and Higbie's theory of surface renewal[28] to explain the form of the equation (Eq. 1) proposed by Kast. By observing that there is no experimental evidence of a physical length scale for the heat transfer, Deckwer postulated that the micro eddy scale of energy dissipation (see Eq. 2) proposed by Kolmogrov is an ideal characteristic length scale for the problem at hand. The author also proposed use of the Kolmogorov velocity (see Eq. 3) as the characteristic velocity.

$$l = \left(\frac{\nu^3}{\varepsilon}\right)^{1/4} \tag{2}$$

$$V = (\nu\varepsilon)^{1/4} \tag{3}$$

The heat transfer correlation (Eq. 4) thus derived by Deckwer had the same form as Kast's model and used a flexible constant.

$$St = c(ReFrPr)^{-0.25} \tag{4}$$

In a separate publication[29], the present authors have described an improved model for predicting the heat transfer rate between the liquid in the column and the coil surface. In this model we (like Deckwer[1]) used Higbie's theory of surface renewal however, with a different

length scale. In fluid elements adjacent to the surface, unsteady heat diffusion takes place and is described by the following equation:

$$\frac{\partial T}{\partial t} = \alpha \frac{\partial^2 T}{\partial x^2} \tag{5}$$

The appropriate boundary conditions to describe this problem are ones that describe the temperature T as the wall temperature T_{coil} at $x = 0$ and all times, the bubble temperature as the initial temperature at all x, and T as the bubble temperature at $x = \infty$ at all times. The final boundary condition is possible only when we approximate the fluid element to have infinite depth and the contact times to be short.

$$T = T_{coil} \qquad x = 0 \qquad t \geq 0 \tag{6}$$

$$T = T_{bubble} \qquad x > 0 \qquad t = 0 \tag{7}$$

$$T = T_{bubble} \qquad x = \infty \qquad t > 0 \tag{8}$$

Solving the above equations, we can obtain the following expression for the heat flux and the thermal resistance.

$$q = \frac{2}{\sqrt{\pi}} \sqrt{\frac{k\rho c_p}{t}} \cdot (T_{bubble} - T_{coil}) \tag{9}$$

$$\frac{1}{R_{bc}} = \frac{2}{\sqrt{\pi}} \sqrt{\frac{k\rho c_p}{t}} \tag{10}$$

From Eq. (10), it is clear that the resistance can be modeled by modeling the surface renewal time (t). For modeling t, we need to model the characteristic length scale and velocity scale accurately. As stated earlier, Deckwer modeled the length and velocity using the Kolmogrov theory (Eqs. 2 & 3). These scales are indicative of the smallest eddies present in the flow and are the scales at which energy is dissipated. These are the scales that form the viscous sub-layer and are very small physically. Hence, this scale is unlikely to regulate

the surface renewal mechanism and the physical mixing. We propose to use a more intuitive length scale which is the integral scale of turbulence.

The integral scale is the representative size of the largest energy bearing eddy. In some cases this scale can be defined by the physical constraints of the flow domain. For example, in pipe flow the diameter of the pipe is of the order of the largest eddies in the flow, and the ratio of the pipe diameter to mean velocity along the pipe is a good estimate of the time period required to describe the flow. In other cases where the integral scale is not obvious from the flow geometry, it can be defined using the autocorrelation of the velocity (i.e., the correlation of a velocity component with itself) as follows:

$$l_{int} = \int_0^\infty \frac{u(x,t) \cdot u(x+r,t)}{u^2} dr \tag{11}$$

where u is the root-mean-square velocity in the x-direction and r is the distance between two points in the flow. The determination of the integral scale using Eq. (11) is not straightforward[30–32]. Direct numerical simulations or large scale visualization experiments using particle image velocimetery or other such techniques are normally used to obtain the autocorrelation of velocity in a 3D flow like in bubble columns[33]. Instead of going into these elaborate techniques, we propose to approximate the integral scale by the bubble diameter. Magaud et al.[34] have presented experimented data that supports this approximation. Similar results concluding that the integral length is of the order of the bubble diameter have been reported by other authors as well[35,36].

We have presented various expressions to calculate the bubble diameter (depending on flow regime) in a previous publication[29]. We use the following expression for the cases involved in this paper[37].

$$D_b = \left\{ \frac{6\sigma d_o}{(\rho_l - \rho_g) \cdot g} \right\}^{1/3} \tag{12}$$

We also propose to use the liquid circulation velocity as the characteristic velocity. This is

logical because the liquid that 'renews' the boundary layer formed on the heat transfer surface is at this velocity and when we aim to calculate the time between two 'renewals' we need to take this into account. Field and Rahimi[38] have proposed that the following expression, which is commonly used in literature[21], is appropriate to calculate liquid circulation velocity in bubble columns.

$$V_c = 1.36 \left\{ gH(V_g - \epsilon \cdot V_b) \right\}^{1/3} \tag{13}$$

According to this expression, the circulation velocity is a function of the bubble velocity and we have previously presented various expressions for calculating the same[29]. An appropriate correlation from the wide selection needs to be picked based on the conditions in the bubble column. For the cases reported in this paper we find it appropriate to use the following equation for evaluating bubble velocity developed based on Mendelson's wave equation[39]. Our own experimental observations showed that this correlation works well for the cases reported in this publication.

$$V_b = \sqrt{\frac{2\sigma}{\rho_l D_b} + \frac{gD_b}{2}} \tag{14}$$

To calculate circulation velocity based on Eq. (13) we also need to evaluate the volumetric gas holdup (ϵ), for which we propose to use the following expression provided by Joshi and Sharma[23]. Several other correlations which have been reported by various researchers, but for the conditions under which we conducted the experiments in (described in Sec. c) we find the following correlation to be the most appropriate. Also, we find that this correlation (Eq. 15) is the most widely used by researchers in the field. Our own experimental observations showed that this correlation works well for the cases reported in this publication.

$$\epsilon = \frac{V_g}{0.3 + 2 \cdot V_g} \tag{15}$$

Based on these expressions, we can evaluate the time between two 'renewals' as $t = \frac{D_b}{V_c}$. By

applying this contact time to Eq. (10), we evaluate the thermal resistance between the liquid in the column and the coil surface. We have previously presented a comparison of the model presented here to the experimental values in literature and there is excellent agreement [29]. This resistance is, however, a minor one in the network and the prediction of the same has little effect on the overall result for the cases reported in this publication.

Thermal resistance between the liquid in the column and the bubbles

The high resistance to diffusion of vapor through a vapor-gas mixture is the reason that regular dehumidifiers have low heat transfer coefficients. In this section, we model the equivalent of the aforementioned diffusion resistance for the case of bubble column dehumidifiers. In Fig. 2, the total heat flux between the bubbles and the liquid was modeled as the sum of the heat flux due to condensation (q_{lt}) and the heat flux due to heat transfer through the resistance $R_{sensible}$. We will evaluate the latent heat using a mass transfer resistance model and the sensible heat using a heat and mass transfer analogy. The mass transfer resistances associated with condensation are shown in Fig. 3. In drawing these resistances it is approximated that the condensation occurs at an interface just outside the bubble surface and mass averaged 'bulk' humidity ratios are defined for the vapor-gas mixture inside the bubble and at the bubble interior surface.

[Figure 3 about here.]

The mass transfer resistances depicted in Fig. 3 are: (1) the resistance to diffusion of vapor through the vapor-gas mixture ($R_{m,1}$) in the bulk (ω_{bulk}) to the bubble surface (ω_{bubble}) and (2) the mass transfer resistance caused by bubble motion through the liquid ($R_{m,2}$). The first resistance is not easy to model without knowing the mechanism of convective transport inside the bubble which could be augmented by a fluid circulation caused by rapid and asymmetric vertical motion of the bubble in the liquid pool. Since there are several complexities involved in evaluating the mechanism of transport inside the bubble, we assume a boundary layer is formed for diffusive transport and approximate the thickness of the boundary layer by the

radius of the bubble itself. This is an upper limit for the size of the boundary layer and the associated thermal resistance and hence, in the succeeding sections (Sec. c) it is shown that the heat transfer and condensation rates predicted by the model consistently underestimates those measured experimentally. The model equation is:

$$k_{l,1} = \frac{D_{AB}}{D_b/2} \tag{16}$$

We model the resistance outside the bubble surface using surface renewal mechanism (similar to that presented in Eqs. (5-10)):

$$k_{l,2} = \frac{2}{\sqrt{\pi}}\sqrt{\frac{D_{AB}}{t}} \tag{17}$$

The surface renewal time (t) in this case is modeled as the ratio of the bubble diameter and the bubble slip velocity. The bubble slip velocity is the relative velocity of the bubble with respect to the circulating liquid. The liquid circulation velocity and the bubble velocity are calculated using the expression presented in Eq. (13) & (14) respectively. The model equation is:

$$t = \frac{D_b}{V_b - V_c} \tag{18}$$

The heat transfer resistance $R_{sensible}$ can be modeled by defining Lewis factor (Le_f) for the vapor-gas system. The Lewis factor appears in the governing equations of simultaneous heat and mass transfer processes (for example, in wet-cooling towers[40] and in cooling coils[41]). Le_f is defined by Eq. (19) and is directly related to Lewis number which is a fluid property:

$$Le_f = \frac{h_t}{k_l\ \rho\ c_{pg}} \tag{19}$$

$$Le_f \cong Le^{2/3}\,[41] \tag{20}$$

$$\approx 0.89 - 0.92 \text{ for air-water systems}\,[42] \tag{21}$$

$$Le = \frac{\alpha}{D_{AB}} \tag{22}$$

where h_t is the heat transfer coefficient associated with $R_{sensible}$, k_l is the mass transfer coefficient associated with the latent heat, and c_{pg} is the specific heat at constant pressure of the vapor-gas mixture:

$$\frac{1}{h_t\ A} = R_{sensible} \tag{23}$$

$$\frac{1}{k_l} = \left(\frac{1}{k_{l,1}} + \frac{1}{k_{l,2}}\right)^{-1} \tag{24}$$

Here, the heat and mass transfer coefficients are defined based on the heat transfer area of the coil surface (A) instead of the bubble surface area. This is because from an engineering perspective, we need to evaluate the coil area required for a certain total heat duty in the bubble column dehumidifier.

Finally, the correlations for heat transfer coefficient for flow inside circular tubes are well known and documented in heat transfer text books[43]. Based on the flow regime inside the coil, we selected appropriate correlations to evaluate R_{coil}.

Evaluation of total heat flux from the resistance model

In the preceeding sections we presented discussed the models for the various thermal resistances in the bubble column dehumidifier (Fig. 2). In this section, we present the equations needed to solve for the total heat flux and all the temperatures in the bubble column dehumidifier.

The heat flux through the network associated with the sum of the bubble column resistance (R_{bc}) and the convection resistance in the coil (R_{coil}) is defined as follows:

$$q = \frac{\dot{Q}}{A} \tag{25}$$

$$= \frac{\theta_1}{R_{bc} + R_{coil}} \tag{26}$$

The associated log mean temperature difference (θ_1) is defined between the liquid column temperature (T_{column}) and the coolant inlet/exit temperatures. It is very important to note

that experimental data in the literature and our own experimental data reported later in this paper (See Sec. c) have shown the liquid in the column is at a constant temperature because of rapid mixing induced by the bubbles. The LMTD is given as follows:

$$\theta_1 = \frac{(T_{column} - T_{coolant,in}) - (T_{column} - T_{coolant,out})}{\ln\left(\frac{T_{column}-T_{coolant,in}}{T_{column}-T_{coolant,out}}\right)} \tag{27}$$

The heat flux can also be expressed as sum of the latent heat of condensation of the vapor from the vapor-air bubbles into the liquid column and the associated sensible heat transfer.

$$q = q_{latent} + q_{sensible} \tag{28}$$

The sensible heat flux is the one associated with the resistance $R_{sensible}$. The heat transfer coefficient associated with this resistance is evaluated using Eq. (19). It is important to note that the area is normalized using the specific interfacial area of the bubbles. We have

$$q_{sensible} = \frac{\theta_2}{R_{sensible}} \tag{29}$$

$$\frac{1}{h_t\ A} = R_{sensible} \tag{30}$$

$$h_t = Le_f \cdot (\rho \bar{c}_{p,g} k_l) \cdot \frac{a_s vol}{A} \tag{31}$$

The specific interfacial area is evaluated using the following widely used expression[37].

$$a_s = \frac{6\epsilon}{D_b} \tag{32}$$

The associated log mean temperature difference is defined between the column temperature and the air inlet/exit temperature:

$$\theta_2 = \frac{(T_{air,in} - T_{column}) - (T_{air,out} - T_{column})}{\ln\left(\frac{T_{air,in}-T_{column}}{T_{air,out}-T_{column}}\right)} \tag{33}$$

The latent heat transfer rate is calculated using the following expression based on mass flux:

$$q_{latent} = j \cdot h_{fg} \tag{34}$$

The mass flux is evaluated by using the mass conversation equation across the bubble column condenser:

$$j = \frac{\dot{m}_{da}}{A}\left(\omega_{in} - \omega_{out}\right) \tag{35}$$

The energy balance between the coolant and the air is written as follows

$$q = \frac{\dot{m}_{coolant} c_{p,coolant}}{A}(T_{coolant,out} - T_{coolant,in}) \tag{36}$$

$$= \frac{\dot{m}_{da}}{A}(h_{air,in} - h_{air,out}) \tag{37}$$

By applying a mass balance on the vapor over a incremental time dt and integrating the same over a the residence time for the bubble in the liquid t_f we obtain the following expression.

$$k_l \cdot a_s = \frac{1}{t_f} \ln\left[\frac{\omega_{in} - \omega_{sat}}{\omega_{out} - \omega_{sat}}\right] \tag{38}$$

Where the bubble residence time t_f is evaluated as the ratio of the liquid height and the bubble velocity:

$$t_f = \frac{H}{V_b} \tag{39}$$

By solving Eqs. (25-39) we can obtain the heat flux and the associated temperatures from the estimated thermal resistance [Eqs. (5-24)].

Solution technique

The equations presented in this section are solved simultaneously using **Engineering Equation Solver (EES)**[44]. Water is used as the coolant in the coils and EES evaluates water properties using the IAPWS (International Association for Properties of Water and Steam) 1995 Formulation[45]. The vapor-gas mixture considered in this paper is moist air and

its properties are evaluated assuming an ideal mixture of air and steam using the formulations presented by[46]. Moist air properties from EES are in close agreement with the data presented in ASHRAE Fundamentals[47] and pure water properties are equivalent to those found in NIST's property package, REFPROP[48]. Dry air properties are evaluated using the ideal gas formulations presented by Lemmon et al.[49].

Experimental details

A laboratory scale test rig was designed and built to study the condensation process from a vapor-air mixture in a bubble column condenser. Figure 4 shows a schematic diagram of the test apparatus used in the study. The apparatus consists of two bubble columns (4) and (9) with dimensions of 12″ (304.8 mm) width × 12″ (304.8 mm) length × 18″ (457.2 mm) height made from transparent PVC sheets of 3/8″ (9.52 mm) thickness. The first column (4) is used to produce moist air for the experiment by passing air through a sparger (3) into hot water. The water in this column is heated by a 1.5 kW submerged electric heater (5). The air is supplied from a compressor and the flow rate is controlled by valve (1) and measured by rotameter (2). The humidified air from the first bubble column flows to the test column (9) where the dehumidification measurements are carried out. Before entering the second column, the flow rate is measured by a rotameter (6), the pressure is measured by a pressure gauge (7), and the dry and wet bulb temperatures are measured with thermocouples T1 and T2 respectively. Air flows into the sparger of the test column (8) where it is cooled and dehumidified using the cold copper coil (10). The copper coil has a pipe diameter of 1/4″ (6.35 mm), a coil height of 6″ (152.4 mm) and a turn diameter of 9″ (228.6 mm). Cold water acting as the coolant flows inside the coil and is pumped from the cooling tank (15) where chilled water coil (16) keeps the temperature inside this tank almost constant. The dry bulb temperature and wet bulb temperature of the outlet air from the second column are measured by thermocouples T3 and T4 respectively. The two columns are provided with a charging and empting valve at the back side (not shown in figure). Cold water from the

cooling water tank (15) is pumped into the copper coil (10). The flow rate of the water is adjusted by the inline valve (11) and the bypass valve (12). The flow rate of water is measured by rotameter (13) and the fine temperature of the water can be adjusted by the inline electric water heater (14). The inlet and outlet water temperature from the copper coil are measured by thermocouples T5 and T6 respectively. The water temperature in the condenser bubble column is measured at two levels using thermocouples T7 and T8.

[Figure 4 about here.]

The sparger (3) of the humidifier bubble column (4) is a cartridge type sparger of 10″ (254 mm) length. The sparger is from Mott corporation made of stainless steel (316LSS) porous pipe of 2″ (50.8 mm) outside diameter and 1/16″ (1.59 mm) thickness. This sparger generates uniform and fine bubble sizes and has a pressure drop less than 13.7 kPa (2 psi). The sparger (8) in the dehumidifier column is made of aluminium box 10″ (254 mm) × 10″ (254 mm) × 1″ (25.4 mm). The top cover of this box is made of an acrylic sheet with a number of holes drilled in it to generate the air bubbles. There are 5 acrylic sheets; each one has different number of holes, hole diameter, and hole pitch as shown in Table 1. The thermocouples used in the apparatus are of K-type are connected to a data logger and a PC. The thermocouples and the data logging system have an uncertainty of ± 0.1°C. The rotameters used for air flow measurements have a range of 0.8 - 8.2 ft^3/min (378 - 3870 cm^3/s) with a least count of ± 0.2 ft^3/min (± 94.4 cm^3/s). The rotameter used for water flow measurement has a range of 0.01 - 0.85 L/min with a least count of 0.01 L/min.

[Table 1 about here.]

In order to study the impact of bubble-on-coil, we designed a set of circular coils to avoid impact and a set of serpentine coils which will facilitate impact. The photographs of the two set of coils are shown in Fig. 5. It may be observed that the circular coil has a turn diameter of 9″ (228.6 mm) and the sparger face area is 8″ (203.2 mm) x 8″ (203.2 mm) which brings the point of inception of the bubble to be vertically away from the coil. This helps minimize

impact. In the serpentine coil, each pass of the coil is deliberately made to cross over the sparger holes maximizing impact. The results are markedly different for the two coils and are reported later on in this paper (see Sec c).

[Figure 5 about here.]

Results and discussion

In this section, we explain the importance of parameters such as superficial velocity, inlet mole fraction of vapor, bubble diameter, liquid height and effect of bubble-on-coil impact on the performance of a bubble column dehumidifier by varying these parameters independently.

The performance parameter of interest is the total heat flux exchanged between the coolant and the air-vapor mixture. Other alternative performance parameters, such as an 'equivalent' heat transfer coefficient, are not strictly correct, in contrast to the situation for a heat exchanger. This is because defining a global value for heat transfer coefficient will involve defining a log mean temperature difference (or another such global parameters for the device in its entirety) between the air and water temperatures at the inlet and outlets. This would amount to associating the mass transfer (and the associated latent heat release, which is the major portion of the total heat exchanged between the fluid streams) with a temperature difference: and this is ofcourse inappropriate because the mass transfer is associated with a concentration difference and not a temperature difference[50–52]. It is, hence, logical to use heat flux as the performance parameter since it captures all the important characteristics of the bubble column dehumidifier (including the condensation rate) but does not involve all of the aforementioned issues.

Effect of superficial velocity

Several researchers have studied the effect of superficial velocity on mass transfer in bubble columns[20,53–56]. These studies, however, did not involve condensation from the bubble into the liquid column. A typical example of the mass transfer studies in literature would be

absorption of isobutylene in aqueous solutions of H_2SO_4[57,58]. Researchers have also separately studied the effect of superficial velocity on heat transfer to immersed surfaces in bubble column reactors[1,24,25,59–64]. However, we should note that the effect of superficial velocity on simultaenous heat and mass exchange with condensation has not been studied before (to the best knowledge of the authors), and it will be the focus of this section.

The general consensus in literature is that the heat and mass transfer coefficients are higher at higher superficial velocity[65]. Studies have also shown that the rate of increase of heat transfer coefficients with gas velocity is more pronounced at lower gas velocity, and more gradual at higher gas velocities. This is because of the change in flow regime from homogenous bubbly flow to the churn-turbulent regime. The effect of increase in superficial velocity is reported to be lower in the churn-turbulent regime.

A flow regime map reported by Shah et al.[20] predicts that the transition velocity for the experimental bubble column reported in the current publication lies somewhere between 4.5 and 7 cm/s (based on an effective column diameter of 30.5 cm). During experimentation it was observed that between superficial velocities of 3 to 8 cm/s the bubble flow was either perfect or imperfect bubbly flow (churn turbulence and slug flow was not observed).

Figure 6 illustrates experimental and calculated values of heat flux at various values of superficial velocity. These results are at fixed values for bubble diameter, inlet mole fraction and water column height. The trend and the slope of the curve presented in Fig. 6 is representative of the trend obtained at other values of the aforementioned fixed parameters. From Fig. 6, it may be observed that as the superficial velocity was increased so was the heat flux which is a conclusion consistent with other such studies in literature. In addition, it can be observed that the predictive model estimates the effect of the superficial velocity accurately.

[Figure 6 about here.]

The uncertainity of measurement on the superficial velocity is $\pm$ 0.11 cm/s and that on the heat flux is $\pm$ 5%.

Effect of bubble diameter

In the literature, no consensus is evident on the effect of bubble diameter on transport coefficients in bubble columns. While on the one hand some researchers have reported that bubble properties (including bubble diameter) affect the mass transfer coefficient greatly[66–68], on the other hand Deckwer[1] has suggested that there is no evidence of the effect of bubble diameter on heat transfer to immersed surfaces. Also, the effect of bubble diameter on simulatenous heat and mass transfer has not been investigated yet.

Our experiments and modeling show (see Fig. 7) that there is a relatively minor but discernible effect of bubble diameter on the total heat flux exchanged in a bubble column dehumidifier. The heat flux is found to decrease with an increase in bubble diameter. This result is found to be consistent at other values of the fixed parameters (superficial velocity, inlet mole fraction and liquid height) as well. It is to be noted that the predictive model proposed in Sec. c predicts the trend in Fig. 7 to a good degree of accuracy.

[Figure 7 about here.]

Effect of inlet mole fraction

In steam condensers with a small amount of non-condensable gas present ($< 10\%$ by mole) the inlet mole fraction of vapor has been reported to have a very sharp effect on the heat transfer coefficient[11,15]. As mentioned earlier (in Sec. c), experimental data in the literature suggests that the effect is almost quadratic in nature. In this section, we investigate the effect of the same parameter in a bubble column dehumidifier.

The inlet mole fraction of vapor is varied from 10% to 25% (3.6 to 9 times lower than regular condensers) at fixed values of superficial velocity, bubble diameter and liquid height. Fig. 8 illustrates the experimental and modeling results for the same. A strong effect of the mole fraction is seen, as is also the case in steam condensers. From our experiments, we observe that the effect is more linear than quadratic (in the studied range). Hence, the presence of non-condensable gas is affecting the heat transfer to a much lesser degree

than in the film condensation situations of a standard dehumidifier. This demonstrates the superiority of the bubble column dehumidifier[69]. This observation is further discussed in Sec. c. Figure 8 also illustrates that the predictive model predicts the effect of inlet mole fraction very accurately.

[Figure 8 about here.]

The uncertainity of measurement on the mole fraction is ± 1%.

Effect of liquid column height

Regular dehumidifiers and steam condensers can be designed to have minimal pressure drop (as low as a few hundred Pa). In bubble columns, a large percentage of the pressure drop that occurs on the vapor side is due to the hydrostatic head of the liquid in the column that the air-vapor mixture has to overcome. Thus, it is desirable to keep the liquid height to a minimum value. The cooling coils must remain fully immersed in the liquid pool, and hence, the minimum liquid height should be that which just immerses the coils.

[Figure 9 about here.]

Figure 9 illustrates that there is no effect of reducing the liquid height from 10″ (254 mm) to 6″ (152.4 mm - the minimum height at which the coil was fully immersed). This can be understood by considering the length scale of the liquid circulation, which we have postulated as the intergral length of turbulence. As explained earlier in Sec. c, the integral length is very close to the bubble diameter. Hence, the scale at which the circulation happens in the liquid is of the order of a millimeter which is two orders of magnitude lower than the liquid height. Therefore, unless the liquid height is reduced to a few millimeters, it will not have an effect on the bubble column performance. This is a very significant consideration when designing bubble column dehumidifiers for systems which cannot take large gas side pressure drops, such as the humidification dehumidification desalination (HDH) system[70,71]. The intricacies of integrating the bubble column dehumidifier with low liquid height in an HDH system are explained in a separate publication[72].

Comparison of model and experiments

We have seen that the predictive model estimates the effect of bubble diameter, superficial velocity and inlet mole fraction of vapor on heat flux exchanged in a bubble column dehumidifier accurately. In Fig. 10 we present a comparison of the experimental data and the model for various boundary conditions in a parity plot. There is excellent agreement (within -20%), and as per our expectation, the model consistently underpredicts the heat flux. This is because we approximated the boundary layer inside the bubble to be of the order of the bubble radius itself (Sec. c), which is clearly an overestimation of the associated thermal resistance.

[Figure 10 about here.]

Effect of bubble-on-coil impact

In consideration of the effect of all of the different parameters (described in the previous paragraphs), bubble-on-coil impact was avoided during experimentation (see Sec. c) and neglected in the predictive model. In this section, we study the effect of impact using the serpentine coils shown in Fig. 5. Figure 11 illustrates this effect. It may be observed that impact raises the heat transfer rates to significantly higher values. Thus, in case of the serpentine coils, a major portion of the heat communicated between the air-vapor bubbles and the coils is through direct impact between the two. Hence, to obtain higher heat transfer rates it is desirable to design coils to have maximum impact.

[Figure 11 about here.]

Comparison with existing devices

A state-of-the-art dehumidifier (which works operates in the film condensation regime) procured from George Fischer LLC was found to yield a maximum heat flux of 1.8 kW/m^2 (as per the design specification) compared to a maximum of 8 kW/m^2 obtained in the bubble column dehumidifier (with high bubble-on-coil impact and a superficial velocity of 7 cm/s)

demonstrating the superior performance of the novel device. This comparison has been carried out at the same inlet conditions for the vapor-air mixture and the coolant streams. Also, the streamwise temperature differences were similar in both the cases.

Concluding remarks

This paper has proposed a novel bubble column vapor-gas condenser (or dehumidifier) for condensation of vapor in the presence of a large percentage of non-condensable gas. The main conclusions are follows.

1. Bubble column dehumidifiers have an order of magnitude higher heat rates than existing state-of-the-art dehumidifiers operating in the film condensation regime.
2. The bubble column should be designed for high superficial velocity, low bubble diameter and maximum bubble-on-coil impact. In order to minimize pressure drop, the liquid height can be kept to a minimum such that the coil is entirely submerged in the liquid. This is possible because the height has no effect on the performance of the device if it is greater than the bubble diameter ($\approx$4-6 mm).
3. The inlet mole fraction of the vapor is found to have a weaker effect on the performance of the device than in a regular dehumidifier (in which the performance deteriorates quadratically with the vapor mole fraction).
4. A physics based predictive heat transfer model based on a thermal resistance circuit to estimate heat flux and temperature profiles in the bubble column condenser has been developed. The experimental data is predicted within -20%. The model accurately predicts the effects of the various parameters on heat flux without incorporating any adjustable parameters.

Acknowledgments

The authors would like to thank the King Fahd University of Petroleum and Minerals for funding the research reported in this paper through the Center for Clean Water and Clean

Energy at MIT and KFUPM. The fourth author would like to thank Massachusetts Institute of Technology for providing him with a Peabody Visiting Professorship which helped him participate in this study.

References

1. Deckwer WD. On mechanism of heat transfer in bubble column reactors. *Chemical Engineering Science*. 1980;35:1341–1346.

2. Colburn AP, Hougen OA. Design of cooler condensers for mixtures of vapors with noncondensing gases. *Industrial and Engineering Chemistry*. 1934;26:1178–1182.

3. Nusselt W. Die oberflachenkondensation des wasserdampfes. *Zeitschrift des Vereins-DeutscherIngenieure*. 1916;60:541–6.

4. Sparrow EM, Eckert ERG. Effects of superheated vapor and noncondensable gases on laminar film condensation. *AIChE Journal*. 1961;7:473–7.

5. Sparrow EM, Minkowycz WJ, Saddy M. Forced convection condensation in the presence of noncondensables and interfacial resistance. *International Journal of Heat and Mass Transfer*. 1967;10:1829–45.

6. Minkowycz WJ, Sparrow EM. Condensation heat transfer in the presence of noncondensables: interfacial resistance, superheating, variable properties, and diffusion. *International Journal of Heat and Mass Transfer*. 1966;9:1125–44.

7. Denny VE, Mills AF, Jusionis VJ. Laminar film condensation from a steam-air mixture undergoing forced flow down a vertical surface. *Journal of Heat Transfer*. 1971;93:297–304.

8. Denny VE, Jusionis VJ. Effects of noncondensable gas and forced flow on laminar film condensation. *International Journal of Heat and Mass Transfer*. 1972;15:315–326.

9. Wang CY, Tu CJ. Effects of non-condensable gas on laminar film condensation in a vertical tube. *International Journal of Heat and Mass Transfer*. 1988;31:2339–45.

10. Kageyama T, Peterson PF, Schrock VE. Diffusion layer modeling for condensation in vertical tubes with noncondensable gases. *Nuclear Engineering and Design*. 1993;141:289–302.

11. Hasanein HA. Steam condensation in the presence of noncondensable gases under forced convection conditions. Ph.D. thesis, Massachusetts Institute of Technology. 1994.

12. Kuhn SZ. Investigation of heat transfer from condensing steam-gas mixture and turbulent films flowing downward inside a vertical tubes. Ph.D. thesis, University of California at Berkeley. 1995.

13. Maheshwari NK, Vijayan PK, Saha D. Effects of non-condensable gases on condensation heat transfer. In: *Proceedings of 4th RCM on the IAEA CRP on Natural Circulation Phenomena*. 2007; .

14. Hasanein HA, Kazimi MS, Golay MW. Forced convection in-tube steam condensation in the presence of noncondensable gases. *International Journal of Heat and Mass Transfer*. 1996;39:2625–2639.

15. Siddique M, Golay MW, Kazimi MS. Local heat transfer coefficients for forced convection condensation of steam in a vertical tube in the presence of air. *Two-Phase Flow and Heat Transfer (3rd ed)*. 1992;197:386–402. ASME, New York.

16. Rao VD, Krishna VM, Sharma KV, Rao PM. Convective condensation of vapor in the presence of a non-condensable gas of high concentration in laminar flow in a vertical pipe. *International Journal of Heat and Mass Transfer*. 2008;51:6090 – 6101.

17. Hamieh BM, Beckman JR, Ybarra MD. Brackish and seawater desalination using a 20 sq. ft. dewvaporation tower. *Desalination*. 2001;140:217–226.

18. Hamieh BM, Beckman JR. Seawater desalination using Dewvaporation technique: experimental and enhancement work with economic analysis. *Desalination*. 2006;195:14–25.

19. Degaleesan S, Dudukovic M, Pan Y. Experimental study of gas-induced liquid-flow structures in bubble columns. *AIChE Journal*. 2001;47:1913–31.

20. Shah YT, Godbole SP, Deckwer WD. Design parameters estimations for bubble column reactors. *AIChE Journal*. 1982;28:353–79.

21. Hulet C, Clement P, Tochon P, Schweich D, Dromard N, Anfray J. Heat Transfer in Two- and Three-Phase Bubble Columns. *International Journal of Chemical Reactor Engineering*. 2009;7:1–93.

22. Kulkarni AV, Joshi JB. Design and selection of sparger for bubble column reactor. Part I: Performance of different spargers. *Chemical engineering research and design*. 2011; 89:1972–85.

23. Joshi JB, Sharma MM. A circulation cell model for bubble columns. *Chemical Engineering Research and Design*. 1979;57a:244–251.

24. Konsetov VV. Heat transfer during bubbling of gas through liquid. *International Journal of Heat and Mass Transfer*. 1966;9:1103–8.

25. Kast W. Analyse des wrmebergangs in blasensulen. *International Journal of Heat and Mass Transfer*. 1962;5:389.

26. Kutateladze SS, Styrikovich MA. *Hydraulics of gas-liquid systems*. Wright-Patterson Air Force Base. 1960.

27. Kolmogorov A. On degeneration of isotropic turbulence in an incompressible viscous liquid. *Doklady Akademiia Nauk SSSR*. 1941;31:538–540.

28. Higbie R. The rate of absorption of a pure gas into a still liquid during a short time of exposure. *Transactions of American Institute of Chemical Engineers*. 1935;35:365–89.

29. Narayan GP, Lam SG, Sharaqawy MH, Lienhard V JH, Das SK. Mechanism of heat transfer in bubble column reactors. 2012. In preparation.

30. Dias NL, Chamecki M, Kan A, Okawa CMP. Study of Spectra, Structure and Correlation Functions and their Implications for the Stationarity of Surface-Layer Turbulence. *Boundary Layer Meteorology*. 2004;110:165–189.

31. Tritton DJ. *Physical Fluid Dynamics*. Oxford University Press. 1988.

32. I'Aglom AM. *Correlation theory of stationary and related random functions, Vol 1: Basic Results*. Springer Verlag. 1987.

33. ONeill PL, Nicolaides D, Honnery D, Soria J. Autocorrelation Functions and the Determination of Integral Length with Reference to Experimental and Numerical Data. *In proceedings of 15th Australasian Fluid Mechanics Conference*. 2004;Paper # AFMC00064:1–3.

34. Magaud F, Souhar M, Wild G, Boisson N. Experimental study of bubble column hydrodynamics. *Chemical Engineering Science*. 2001;56:4597–4607.

35. Souhar M. Some turbulence quantities and energy spectrain the wall region in bubble flows. *Physics of Fluids A*. 1989;1:1558–65.

36. Lance M, Bataille J. Turbulence in the liquid phase of a uniform bubbly air-water flow. *Journal of Fluid Mechanics*. 1991;222:95–118.

37. Miller DN. Scale-up of agitated vessels gas-liquid mass transfer. *AIChE Journal*. 1974; 20:445–53.

38. Field RW, Rahimi R. Hold-up heat transfer in bubble columns. In: *Fluid Mixing III*. European Federation of Chemical Engineering, Amarousion-Pefki, Greece. 1988; pp. 257 – 270.

39. Mendelson HD. The Prediction of Bubble Terminal Velocities from Wave Theory. *AIChE Journal*. 1967;13:250.

40. Merkel F. Verdunstungskhlung. *VDI-Zeitchrift*. 1925;70:123–8.

41. Threlkeld JL. *Thermal environmental engineering*. Prentice-Hall Inc. 1970.

42. Bosnjakovic F. *Technische Thermodinamik*. Theodor Steinkopf, Dresden. 1965.

43. Lienhard V JH, Lienhard IV JH. *A Heat Transfer Textbook*. 4th ed., Dover Publication, Minoela NY. 2011.

44. Klein SA. Engineering Equation Solver, Academic Professional, Version 8. 2009. URL http://www.fchart.com/

45. Pruss S, Wagner W. The IAPWS formulation 1995 for the thermodynamic properties of ordinary water substance for general and scientific use. *Journal of Physical and Chemical Reference Data*. 2002;31:387–535.

46. Hyland RW, Wexler A. Formulations for the Thermodynamic Properties of Dry Air from 173.15 K to 473.15 K, and of Saturated Moist Air From 173.15 K to 372.15 K, at Pressures to 5 MPa. *ASHRAE Transactions*. 1983b;Part 2A (RP-216)(2794):520–535.

47. Wessel DJ. *ASHRAE Fundamentals Handbook 2001 (SI Edition)*. American Society of Heating, Refrigerating, and Air-Conditioning Engineers. 2001.

48. Lemmon EW, Huber ML, McLinden MO. NIST Standard Reference Database 23: Reference Fluid Thermodynamic and Transport Properties. *Tech. rep.*, REFPROP. Version 8.0 (2007).

49. Lemmon EW, Jacobsen RT, Penoncello SG, Friend DG. Thermodynamic Properties of Air and Mixtures of Nitrogen, Argon, and Oxygen From 60 to 2000 K at Pressures to 2000 MPa. *Journal of Physical and Chemical Reference Data*. 2000;29(3):331–385.

50. Thiel GP, Lienhard V JH. Entropy generation in condensation in the presence of high concentrations of noncondensable gases. 2012. Submitted for Review.

51. Narayan GP, Mistry KH, Sharqawy MH, Zubair SM, V JHL. Energy effectiveness of simultaneous heat and mass exchange devices. *Frontiers in Heat and Mass Transfer*. 2010;1:1–13.

52. Narayan GP, Lienhard V JH, Zubair SM. Entropy generation minimization of combined heat and mass transfer devices. *International Journal of Thermal Sciences*. 2010;49:2057–66.

53. Schumpe A, Grund G. The gas disengagement technique for studying gas holdup structure in bubble columns. *Candian Journal of Chemical Engineering*. 1986;64:891–6.

54. Ozturk SS, Schumpe A, Deckwer WD. Organic liquids in a bubble column: holdups and mass transfer coefficients. *AIChE Journal*. 1987;33:1473–80.

55. Akita K, Yoshida F. Gas hold-up and volumetric mass transfer coefficients in bubble columns. *Industrial and Engineering Chemistry Process Design and Development*. 1973; 12:76–80.

56. Kang Y, Cho YJ, Woo KJ, Kim SD. Diagnosis of bubble distribution and mass transfer in pressurized bubble columns with viscous liquid medium. *Chemical Engineering Science*. 1999;54:4887.

57. Gehlawat JK, Sharma MM. Absorption of isobutylene in Aqueous Solutions of Sulfuric Acid. *Chemical engineering science*. 1968;23:1173.

58. Kroper H, Schlomer K, Weitz HM. How BASF Extracts Isolentylene. *Hydrocarbon Process*. 1969;195:1.

59. Hikita H, Asal S, Kikukawa H, Zalke T, Ohue M. Heat transfer coefficients in bubble column. *Industrial and Engineering Chemistry Process Design and Development*. 1981; 20:540–5.

60. Kawase Y, Moo-Young M. Heat transfer in bubble column reactors with Newtonian and non-Newtonian fluids. *Chemical Engineering Research and Design*. 1987;65:121–6.

61. Kato Y, Uchida K, Kago T, Morooka S. Liquid holdup and heat transfer coeffcient between bed and wall in liquid-solid and gas-liquid-solid fluidized beds. *Powder Technology*. 1981;28:173–9.

62. Cho YJ, Woo KJ, Kang Y, Kim SD. Dynamic characteristics of heat transfer coeffcient in pressurized bubble columns with viscous medium. *Chemical Engineering and Processing*. 2002;41:699–706.

63. Saxena SC, Rao NS, Saxena AC. Heat-transfer and gas-holdup studies in a bubble column: air-water-glass bead system. *Chemical Engineering Communications*. 1990;96:31–55.

64. Li H, Prakash A. Heat transfer and hydrodynamics in a three-phase slurry bubble column. *Industrial and Engineering Chemistry research*. 1997;36:4688–94.

65. Kantarci N, Borak F, Ulgen KO. Bubble column reactors. *Process Biochemistry*. 2005; 40:226383.

66. Fukuma M, Muroyama K, Morooka S. Properties of bubble swarm in a slurry bubble column. *Journal of Chemical Engineering of Japan*. 1987;20:28–33.

67. Krishna R, Baten JMV. Mass transfer in bubble columns. *Catalysis Today*. 2003;79-80:67–75.

68. Behkish A, Men Z, Inga RJ, Morsi BI. Mass transfer characteristics in a large-scale slurry bubble column reactor with organic liquid mixtures. *Chemical Engineering Science*. 2002; 57:3307–24.

69. Narayan GP, Thiel GP, McGovern RK, Sharaqawy MH, Lienhard V JH. Multi-Stage Bubble Column Dehumidifier. patent pending, USSN # 13/241,907.

70. Narayan GP, Sharqawy MH, Summers EK, Lienhard V JH, Zubair SM, Antar MA. The potential of solar-driven humidification-dehumidification desalination for small-scale decentralized water production. *Renewable and Sustainable Energy Reviews*. 2010;14:1187–1201.

71. Narayan GP, Sharqawy MH, Lienhard V JH, Zubair SM. Thermodynamic analysis of humidification dehumidification desalination cycles. *Desalination and Water Treatment*. 2010;16:339–353.

72. Narayan GP, Lam SG, Sharaqawy MH, Das SK, Lienhard V JH. Multi-stage bubble column dehumidifier for low-cost humidification dehumidification desalination systems. 2012. In preparation.

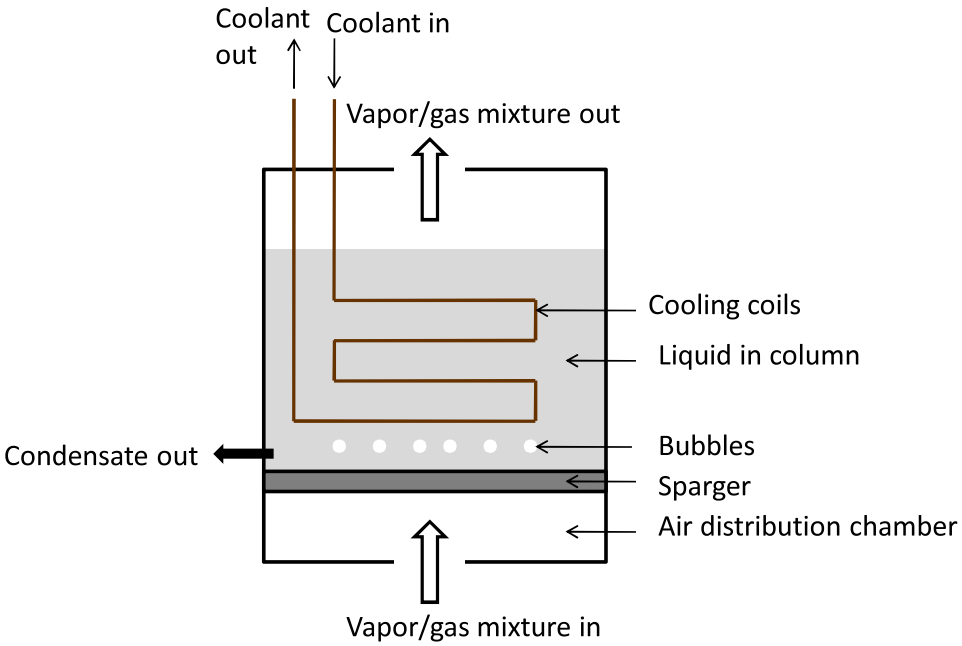

Figure 1: Schematic diagram of the bubble column dehumidifier.

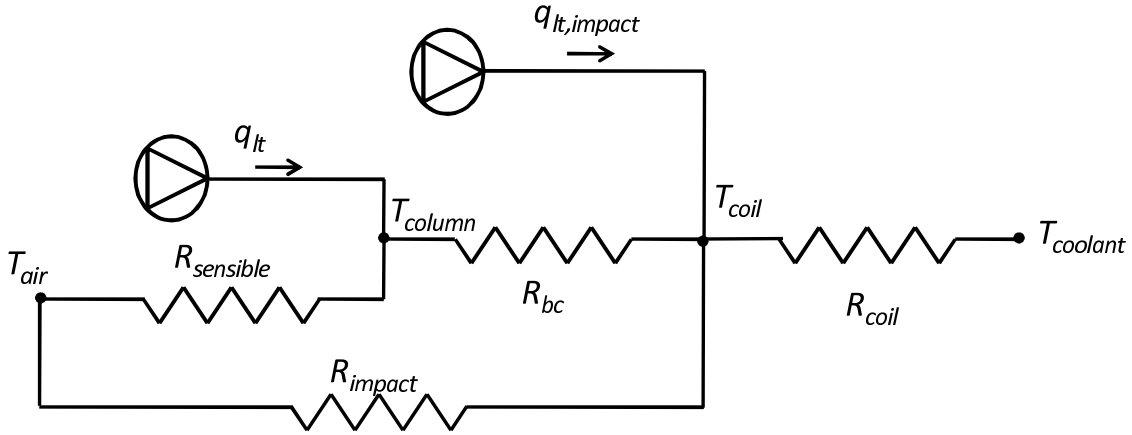

Figure 2: A thermal resistance model for the bubble column dehumidifier.

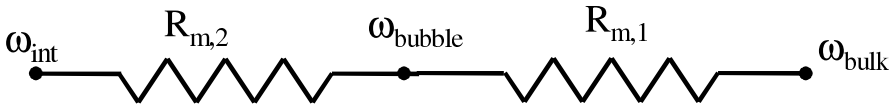

Figure 3: A mass transfer resistance model between the liquid in the column and the bubbles

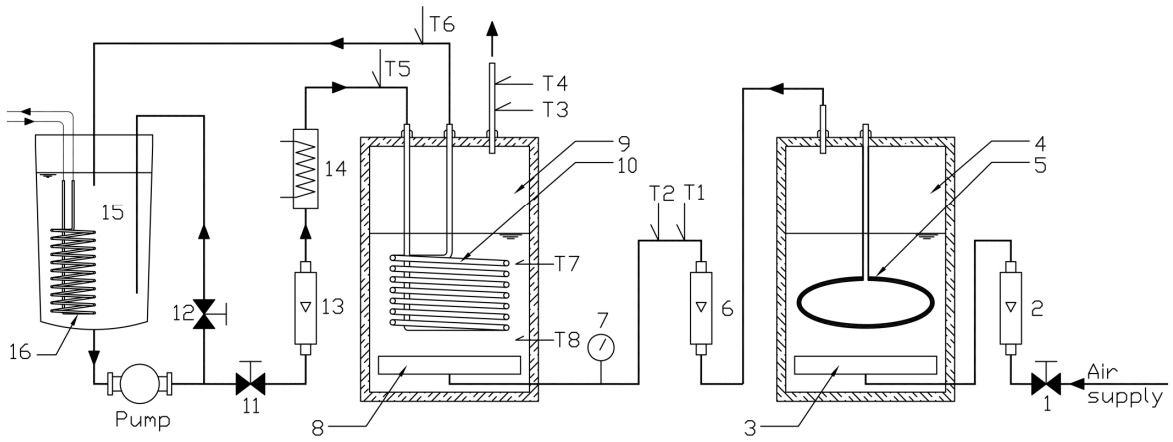

Figure 4: Schematic diagram of test apparatus; (1, 11, 12) valves, (2, 6, 13) rotameter, (3, 8) sparger, (4) humidifier column, (5) submerged electric heater, (7) pressure gauge, (9) dehumidifier column, (10) water coil, (14) inline water heater, (15) cooling water tank, (16) chilled water coil, (T1 – T8) thermocouples

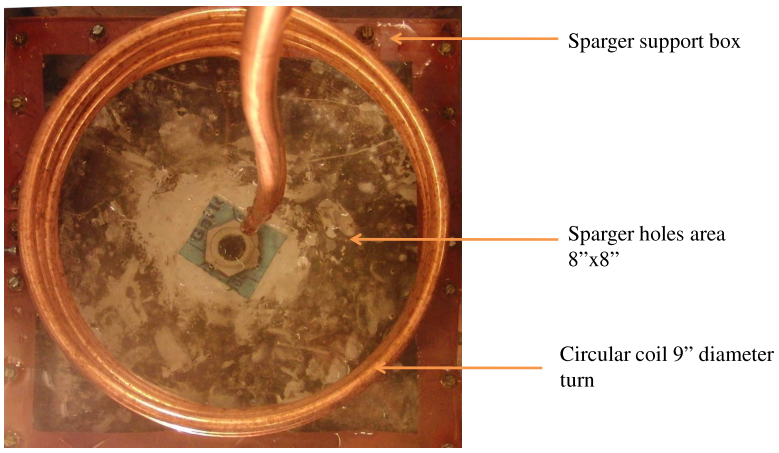

(a) Without impact

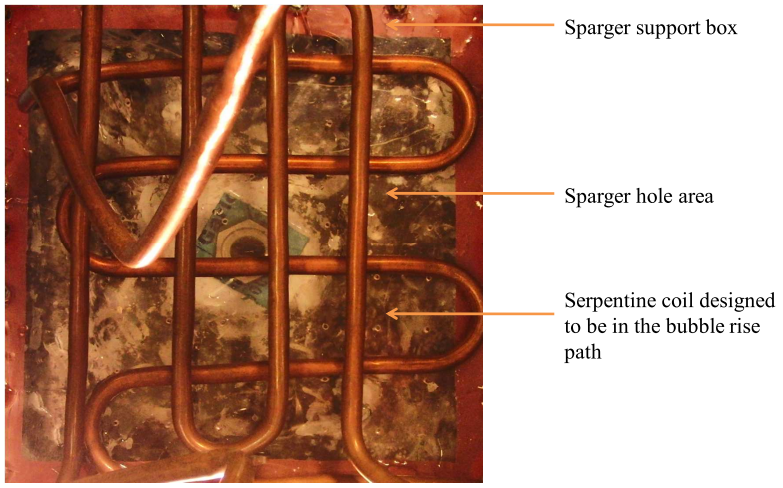

(b) With impact

Figure 5: Photographs showing design of sparger and coil for (a) non-impact and (b) impact cases

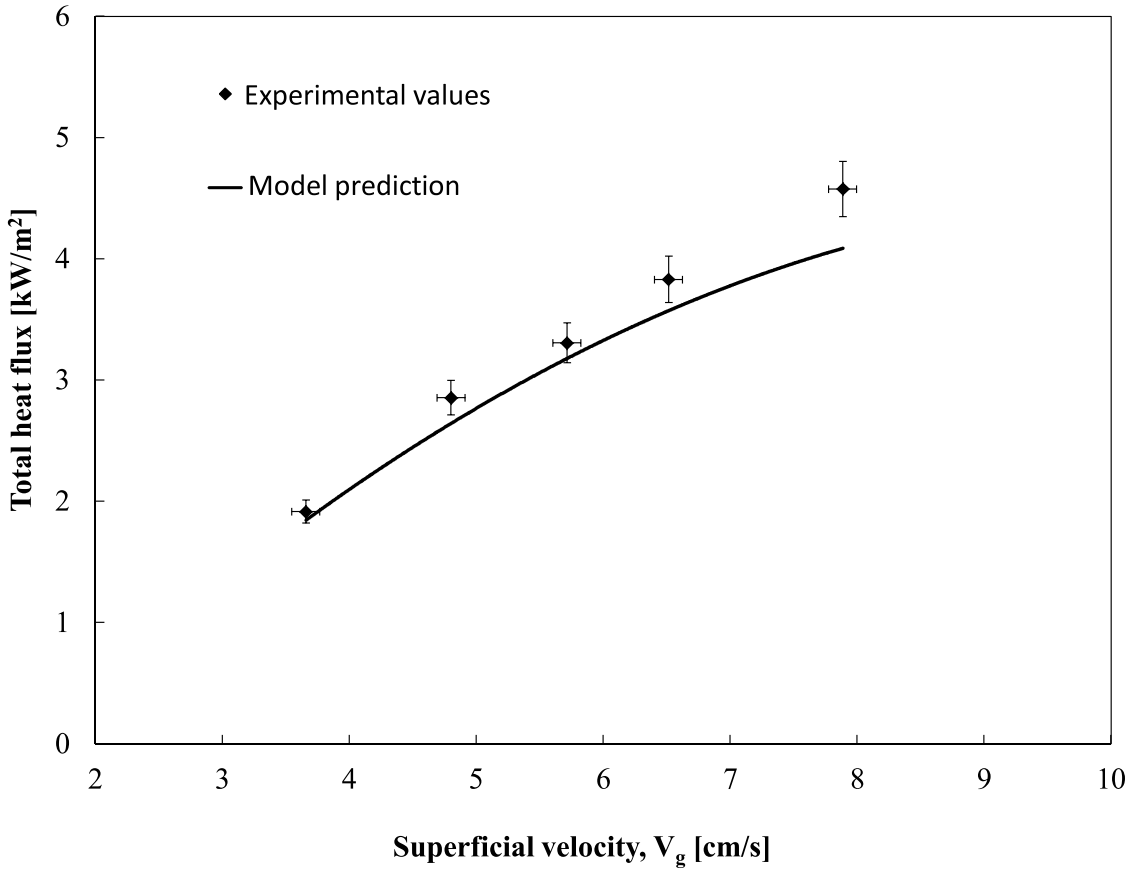

Figure 6: Effect of superficial velocity on the total heat flux in the bubble column measured and evaluated at $D_b = 4\,\mathrm{mm}; \chi_{in} = 21\%;\ H = 254\,\mathrm{mm}$.

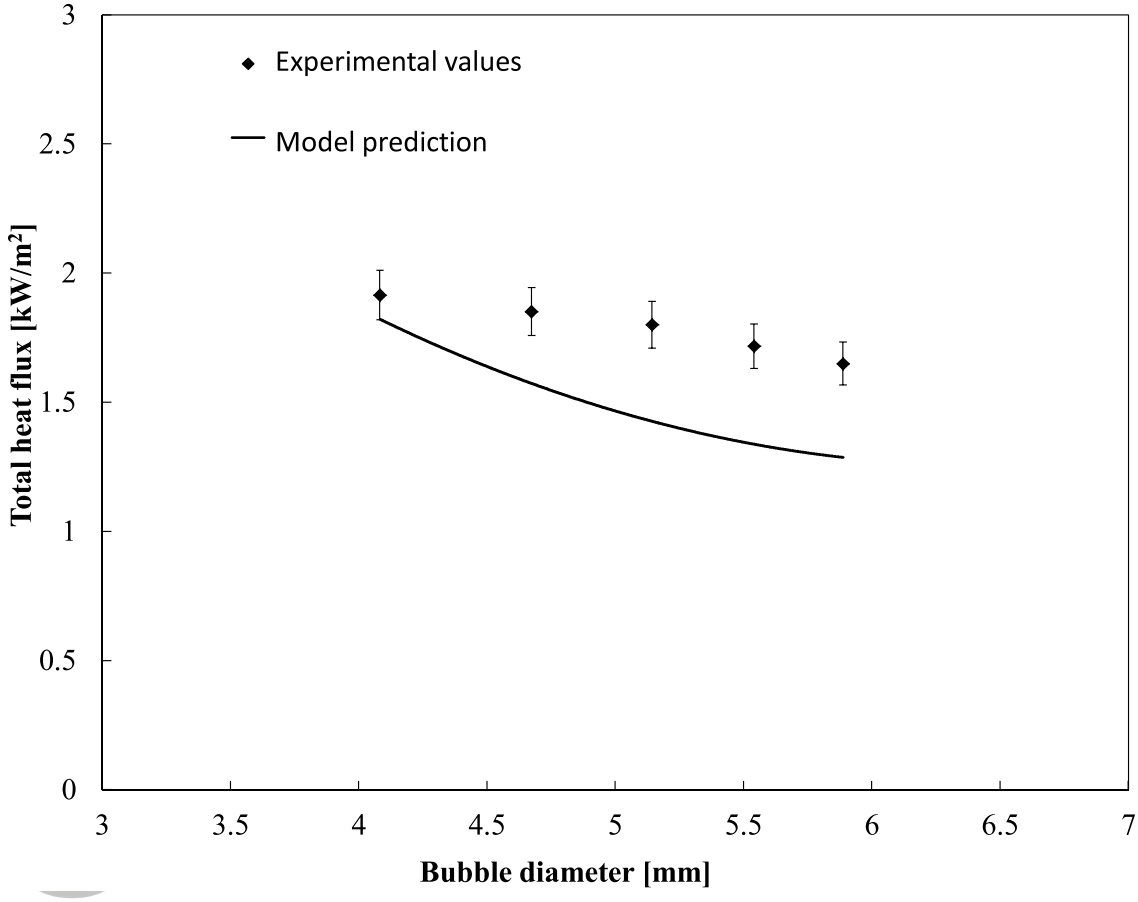

Figure 7: Effect of bubble diameter on the total heat flux in the bubble column measured and evaluated at $V_g = 3.8\,\mathrm{cm/s}$; $\chi_{in} = 21\%$; $H = 254\,\mathrm{mm}$.

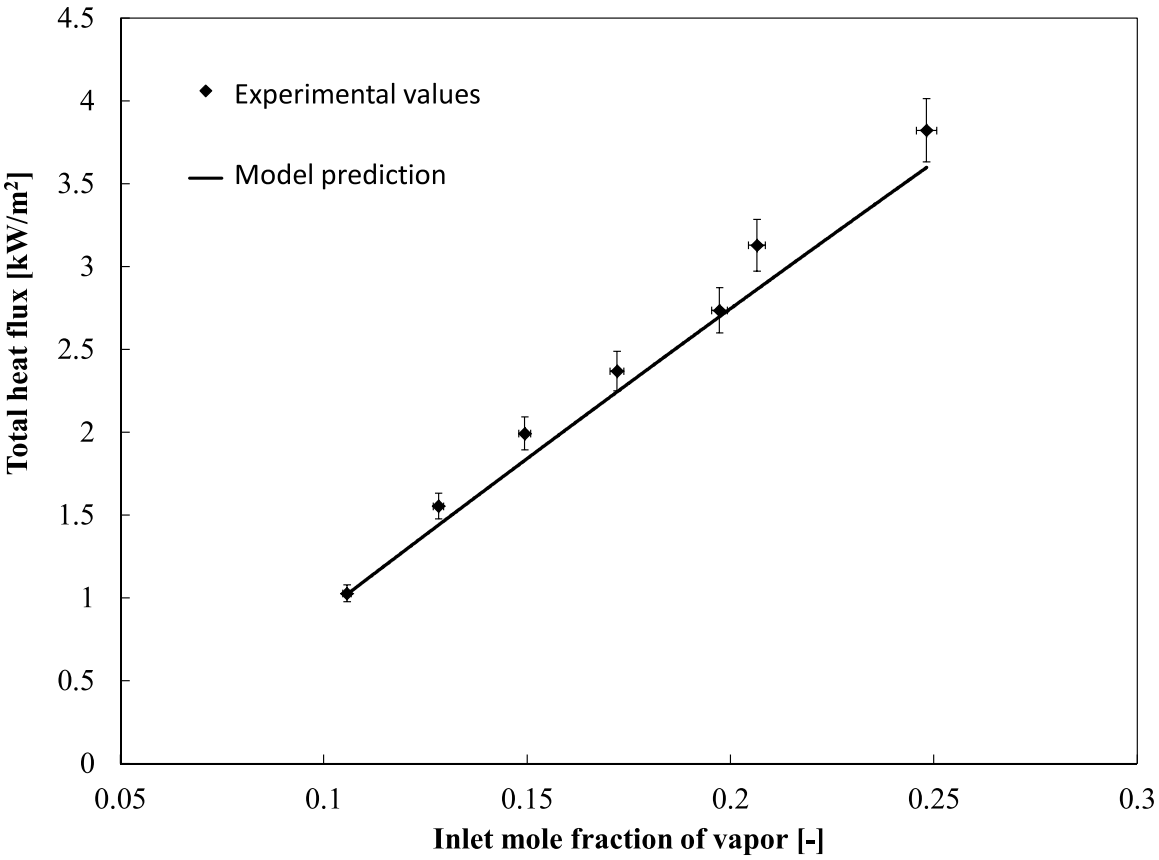

Figure 8: Effect of inlet mole fraction of the vapor on the total heat flux in the bubble column measured and evaluated at $V_g = 3.8\,\mathrm{cm/s}$; $D_b = 4\,\mathrm{mm}$; $H = 254\,\mathrm{mm}$.

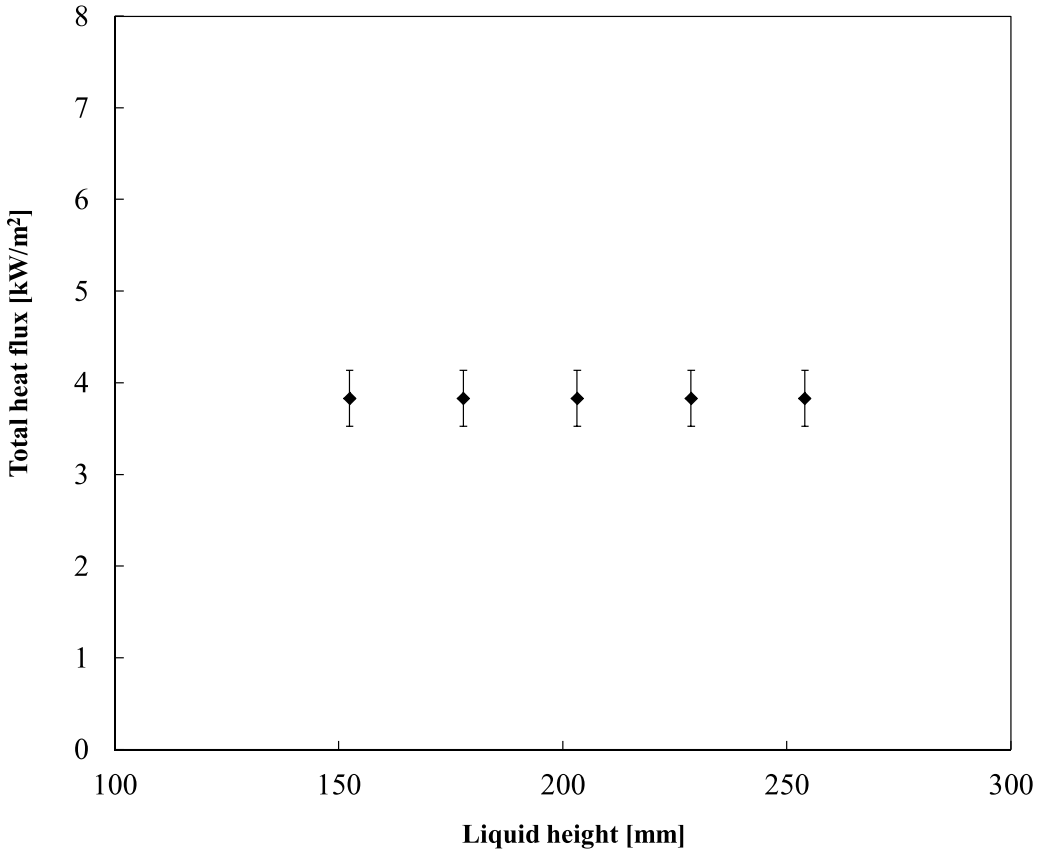

Figure 9: Effect of liquid height on the total heat flux in the bubble column measured and evaluated at $V_g = 6.52\,\mathrm{cm/s}; D_b = 4\,\mathrm{mm};\ \chi_{in} = 21\%$.

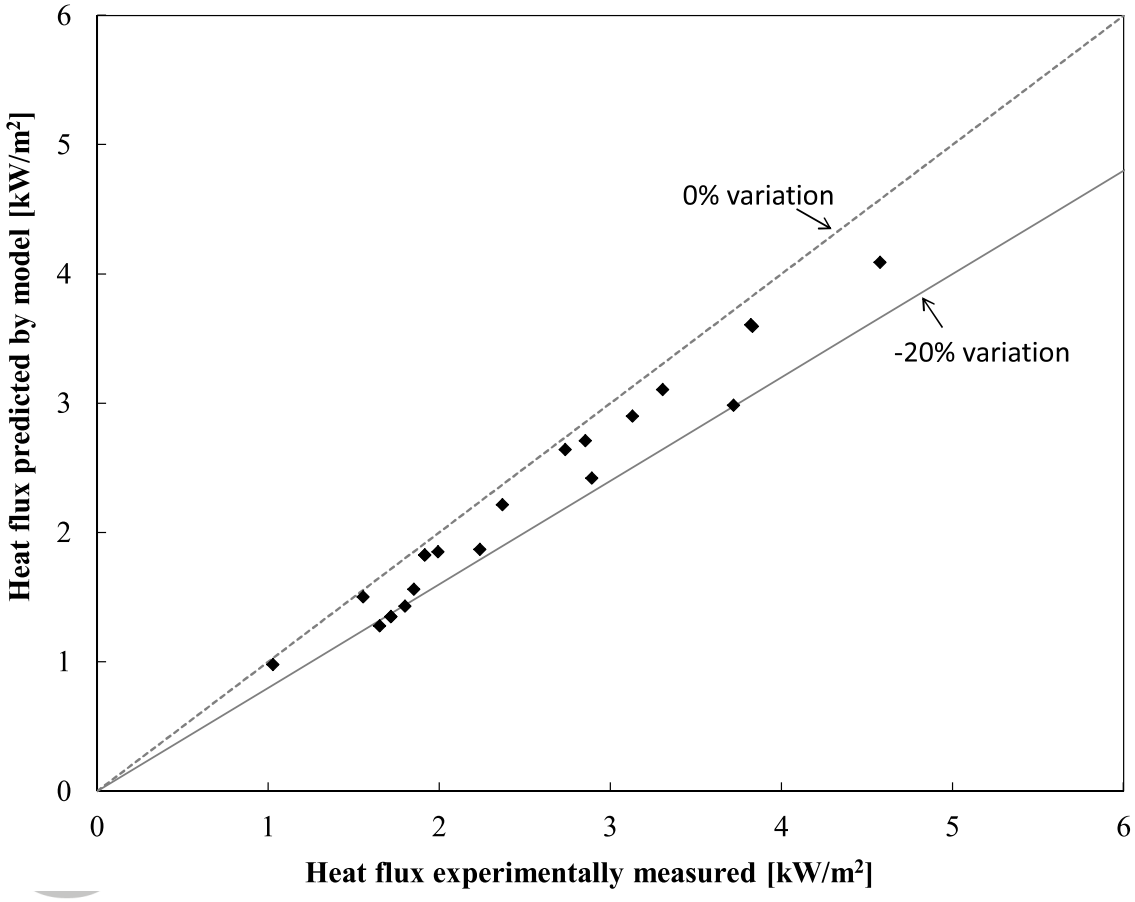

Figure 10: Parity plot of heat flux values evaluated by the model and that measured by experiments for various boundary conditions.

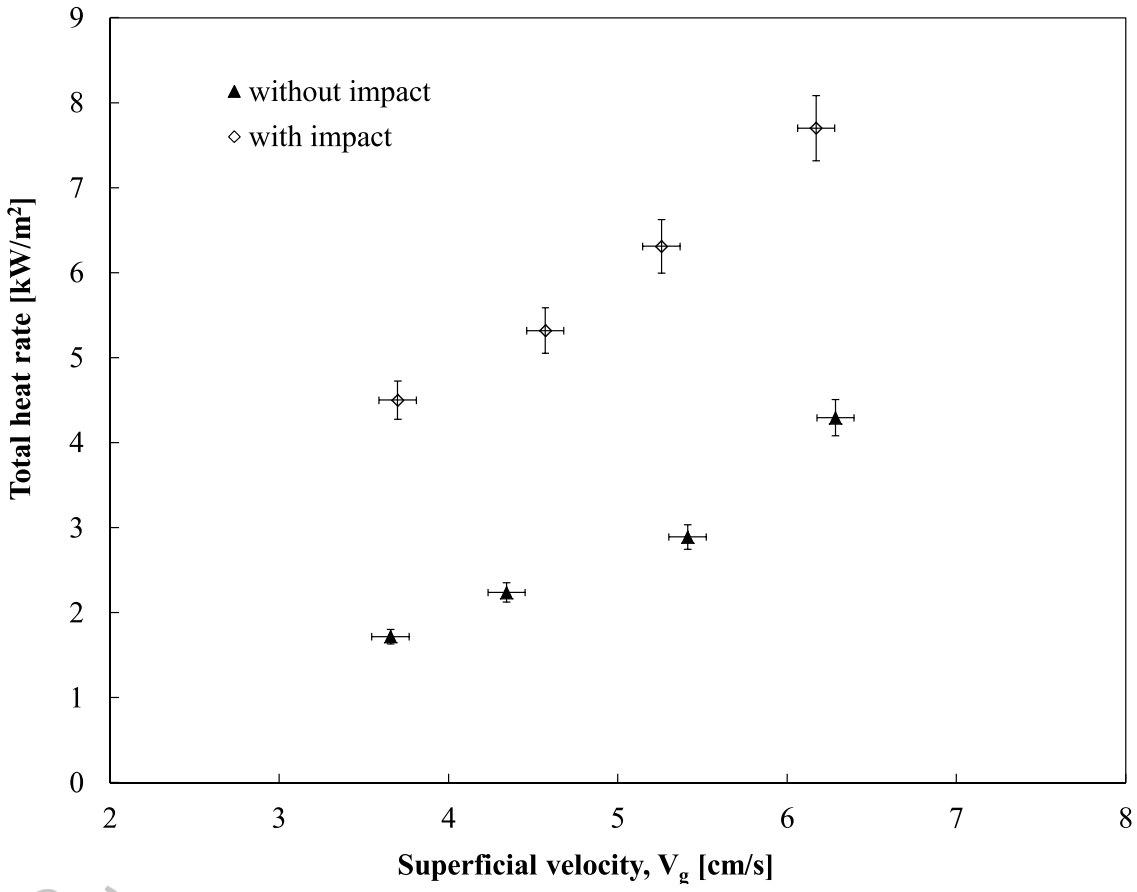

Figure 11: Effect of bubble-on-coil impact.

Table 1: Sparger design

Design No.	Hole size (mm)	Pitch (mm)	Number of holes
1	1.59	16	121
2	2.38	23	64
3	3.18	26	36
4	3.96	32	25
5	4.76	40	16

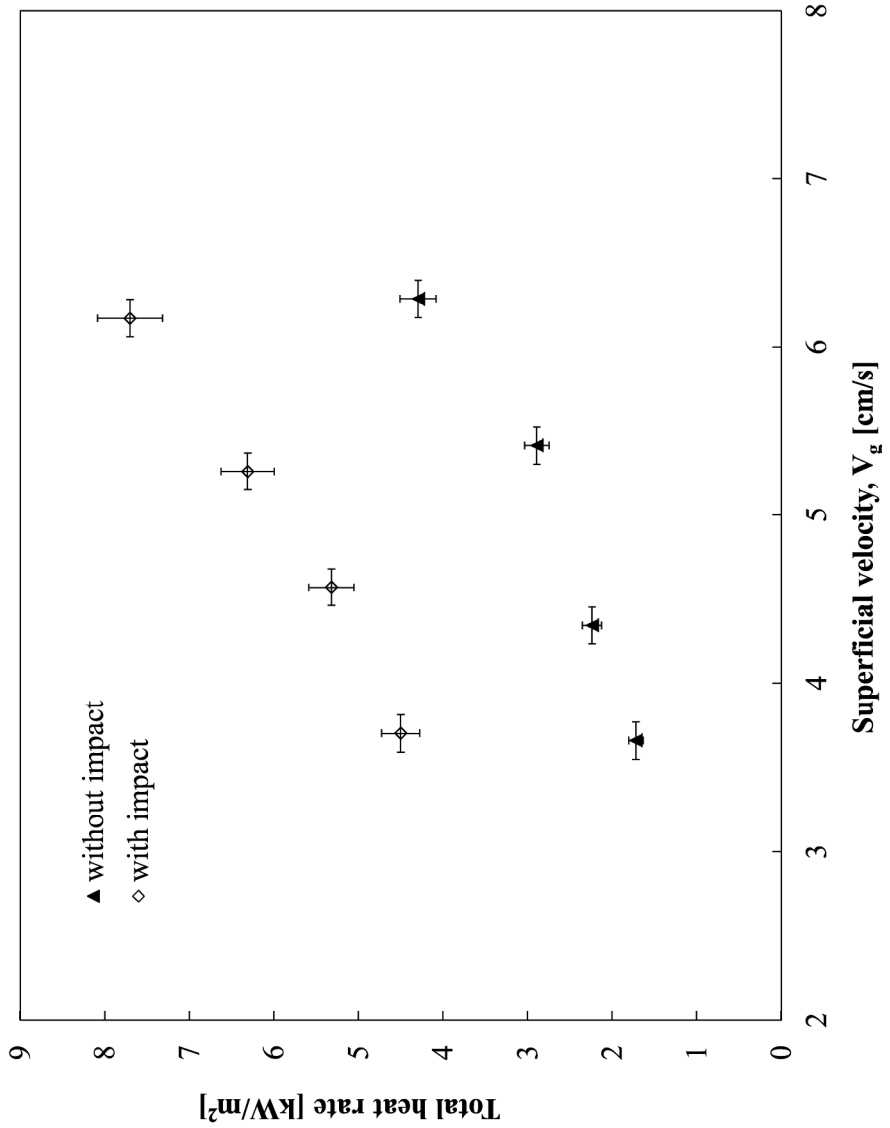

Effect of bubble-on-coil impact.
254x338mm (300 x 300 DPI)

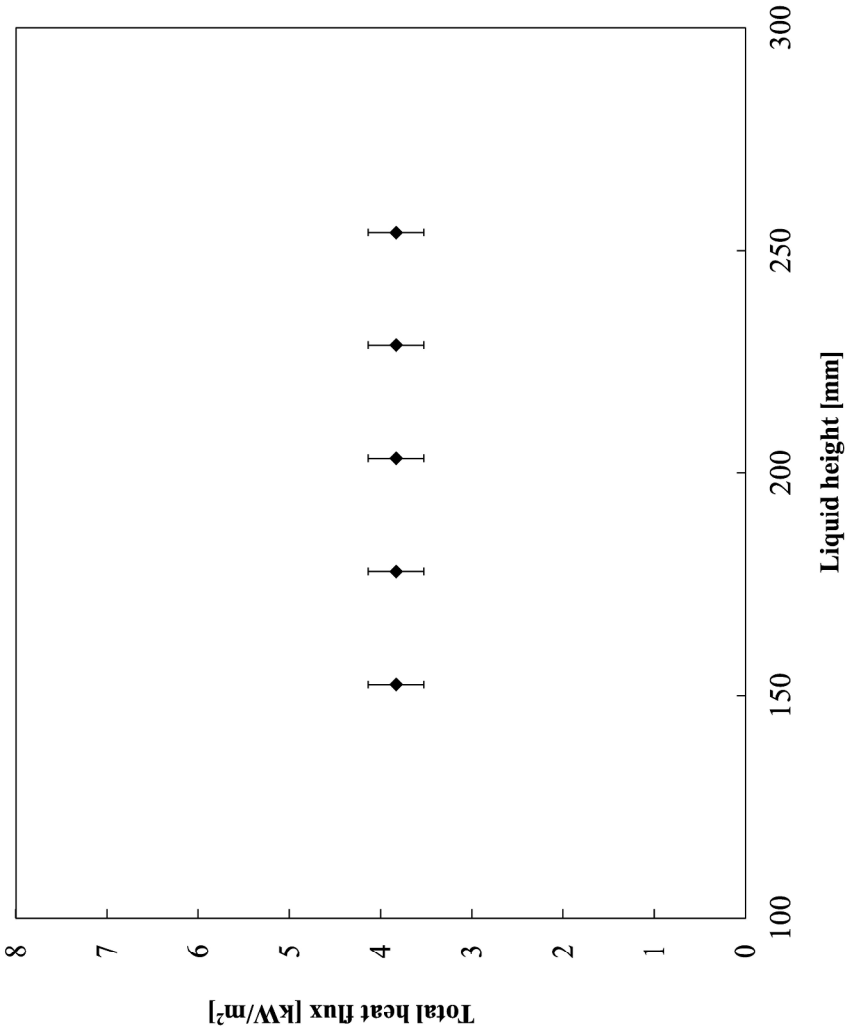

Effect of liquid height on the total heat flux in the bubble column measured and evaluated at $V_{g}=6.52 \hspace{2pt}\rm{cm/s}$;\hspace{2pt}$D_{b}=4\hspace{2pt}\rm{mm};\hspace{2pt} \hspace{2pt}\it{\chi_{in}} = \rm{21}\%$.
254x338mm (300 x 300 DPI)

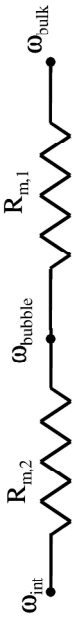

A mass transfer resistance model between the liquid in the column and the bubbles.
254x338mm (300 x 300 DPI)

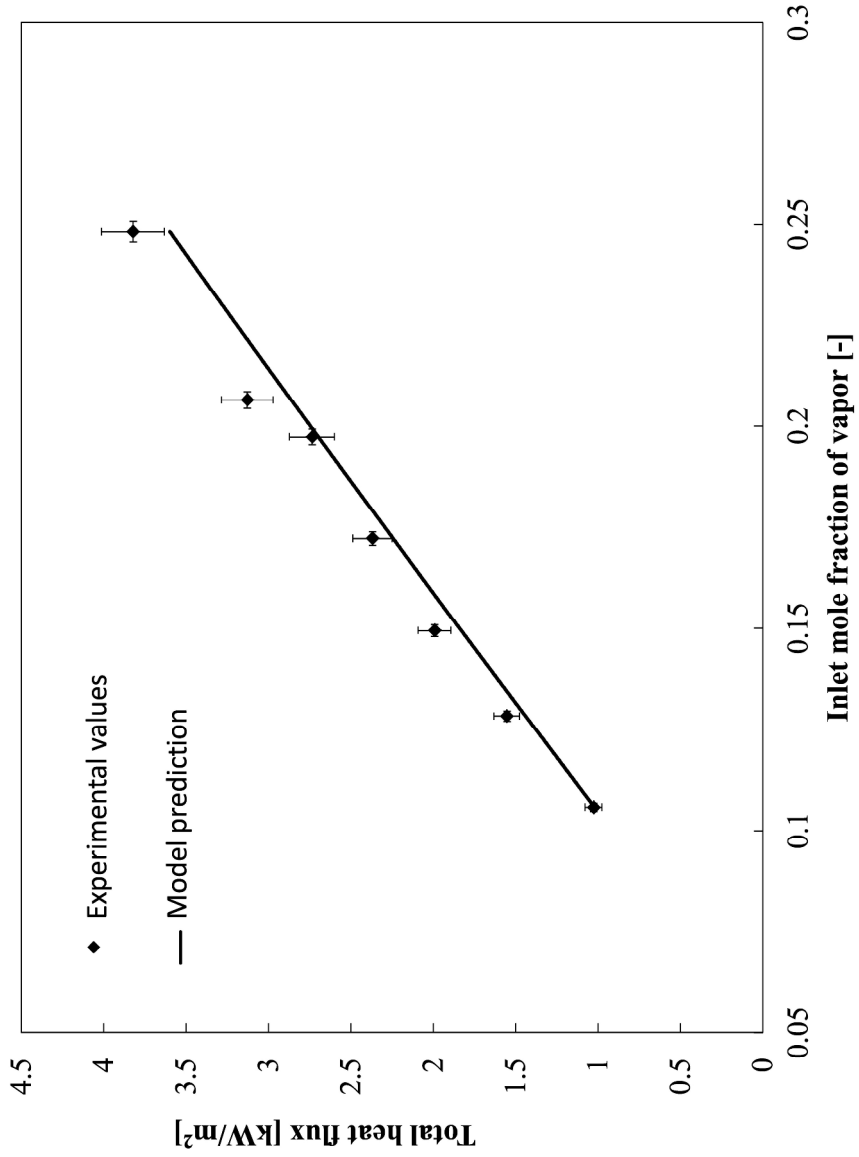

Effect of inlet mole fraction of the vapor on the total heat flux in the bubble column measured and evaluated at $V_{g}=3.8 \hspace{2pt}\rm{cm/s}$;\hspace{2pt}$D_{b}=4\hspace{2pt}\rm{mm};\hspace{2pt} \it{H}=\rm{254}\hspace{2pt}\rm{mm}$.
266x355mm (300 x 300 DPI)

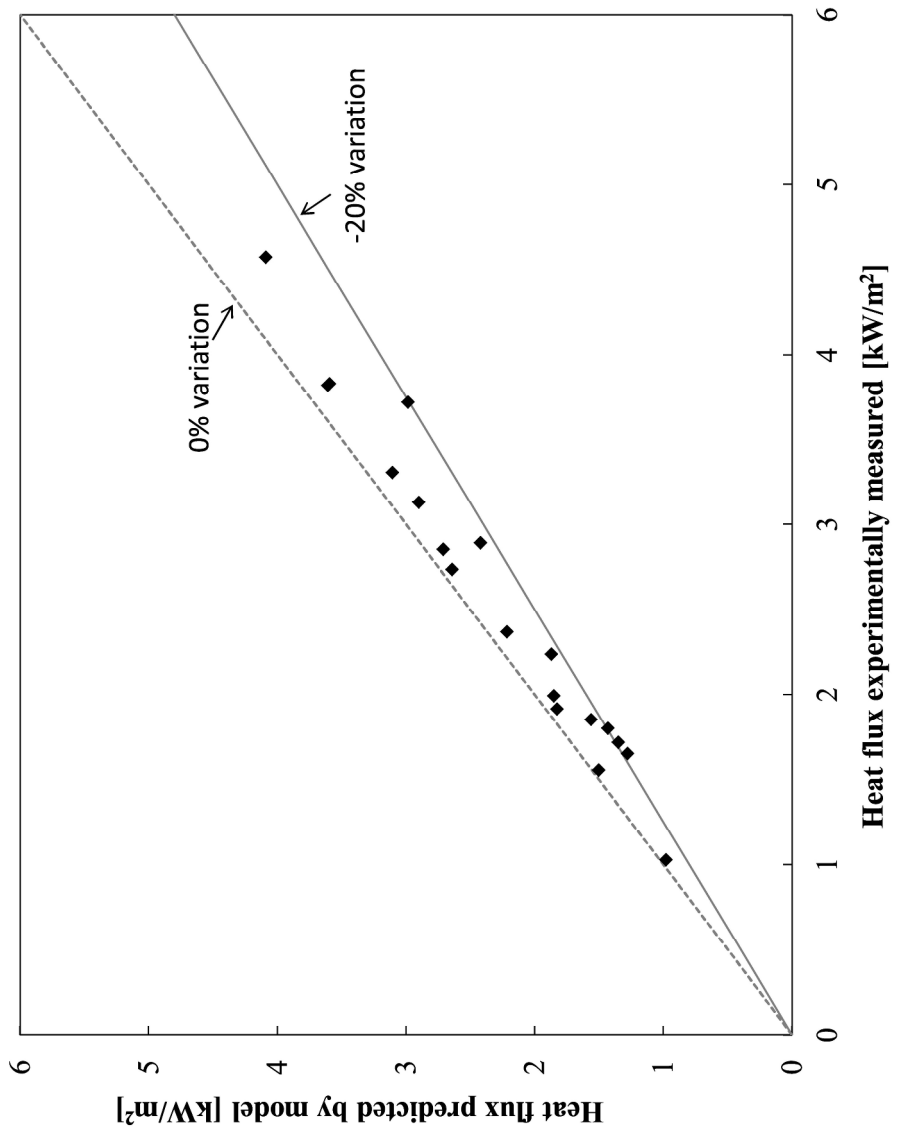

Parity plot of heat flux values evaluated by the model and that measured by experiments for various boundary conditions.
254x338mm (300 x 300 DPI)

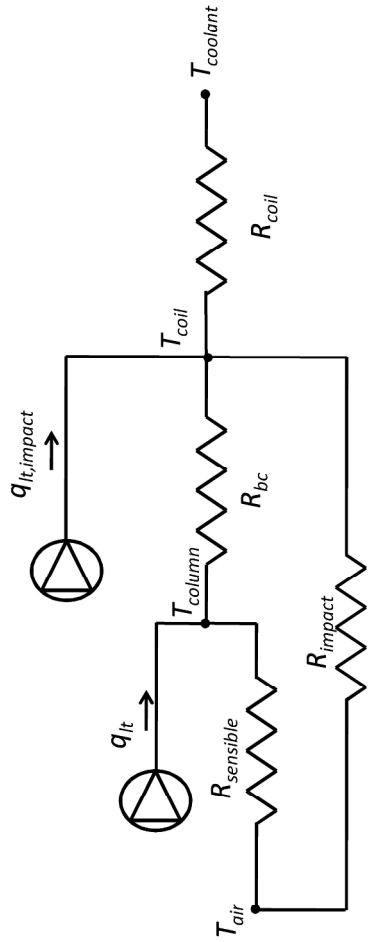

A thermal resistance model for the bubble column dehumidifier.
254x338mm (300 x 300 DPI)

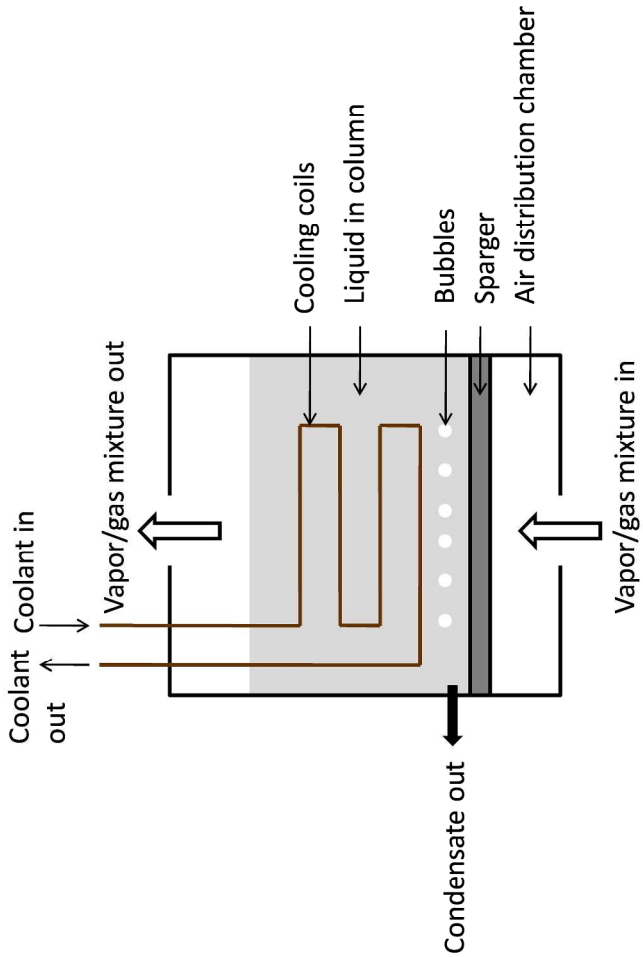

Schematic diagram of the bubble column dehumidifier.
254x338mm (300 x 300 DPI)

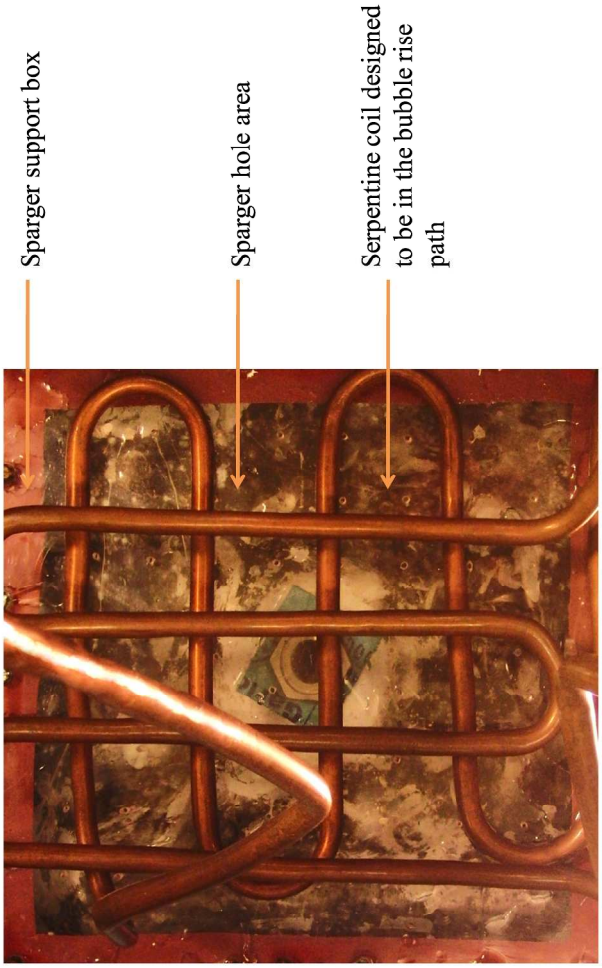

Photographs showing design of sparger and coil for (a) non-impact and (b) impact cases
254x338mm (300 x 300 DPI)

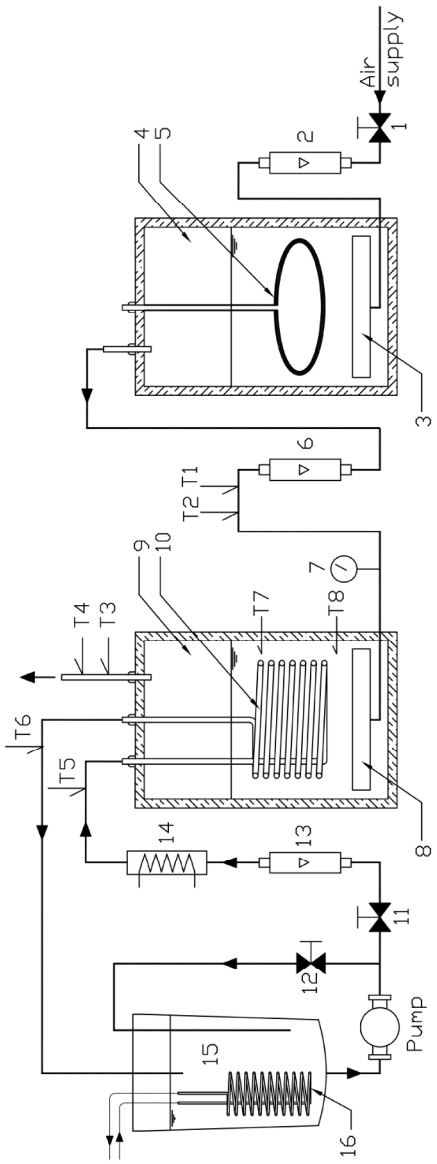

Schematic diagram of test apparatus; (1, 11, 12) valves, (2, 6, 13) rotameter, (3, 8) sparger, (4) humidifier column, (5) submerged electric heater, (7) pressure gauge, (9) dehumidifier column, (10) water coil, (14) inline water heater, (15) cooling water tank, (16) chilled water coil, (T1 -- T8) thermocouples
254x338mm (300 x 300 DPI)

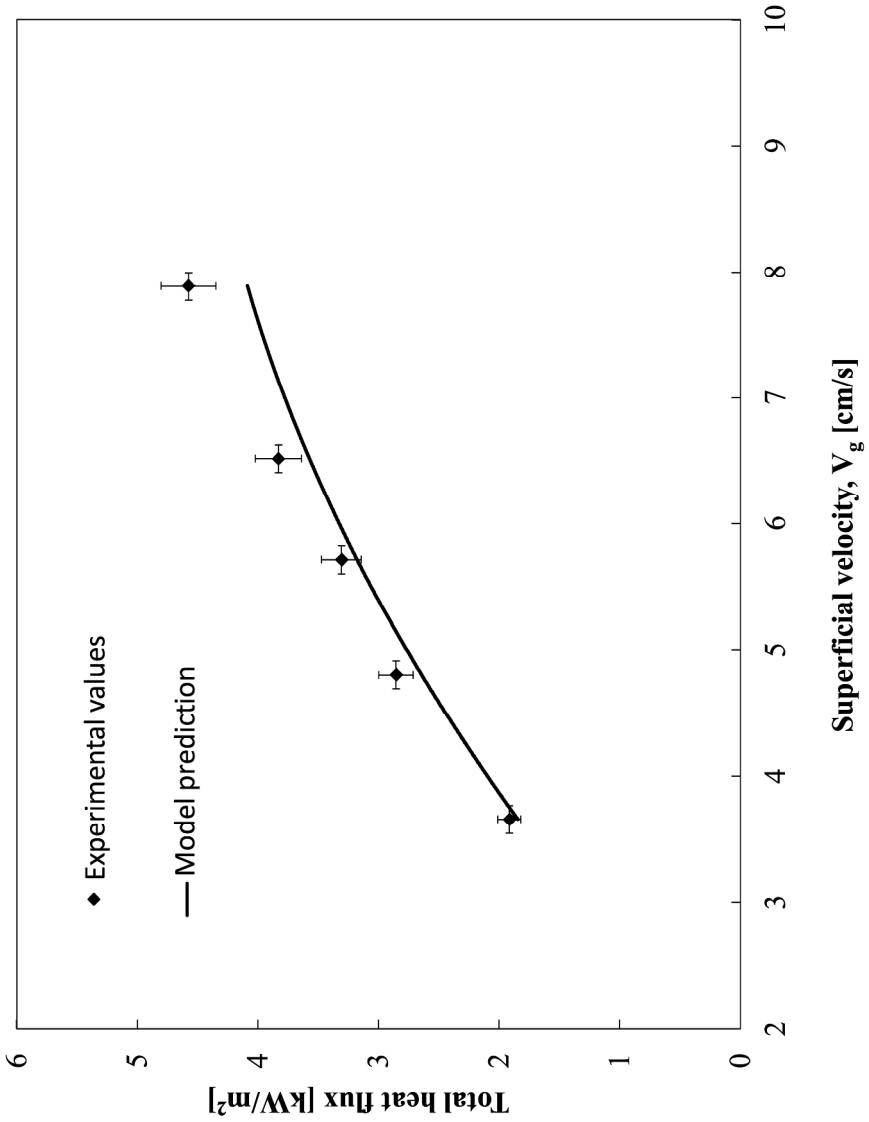

Effect of superficial velocity on the total heat flux in the bubble column measured and evaluated at $D_{b}=4 \hspace{2pt}\rm{mm}$;\hspace{2pt}$\it{\chi_{in}} = \rm{21}\%;\hspace{2pt} \it{H}=\rm{254}\hspace{2pt}\rm{mm}$.
266x355mm (300 x 300 DPI)

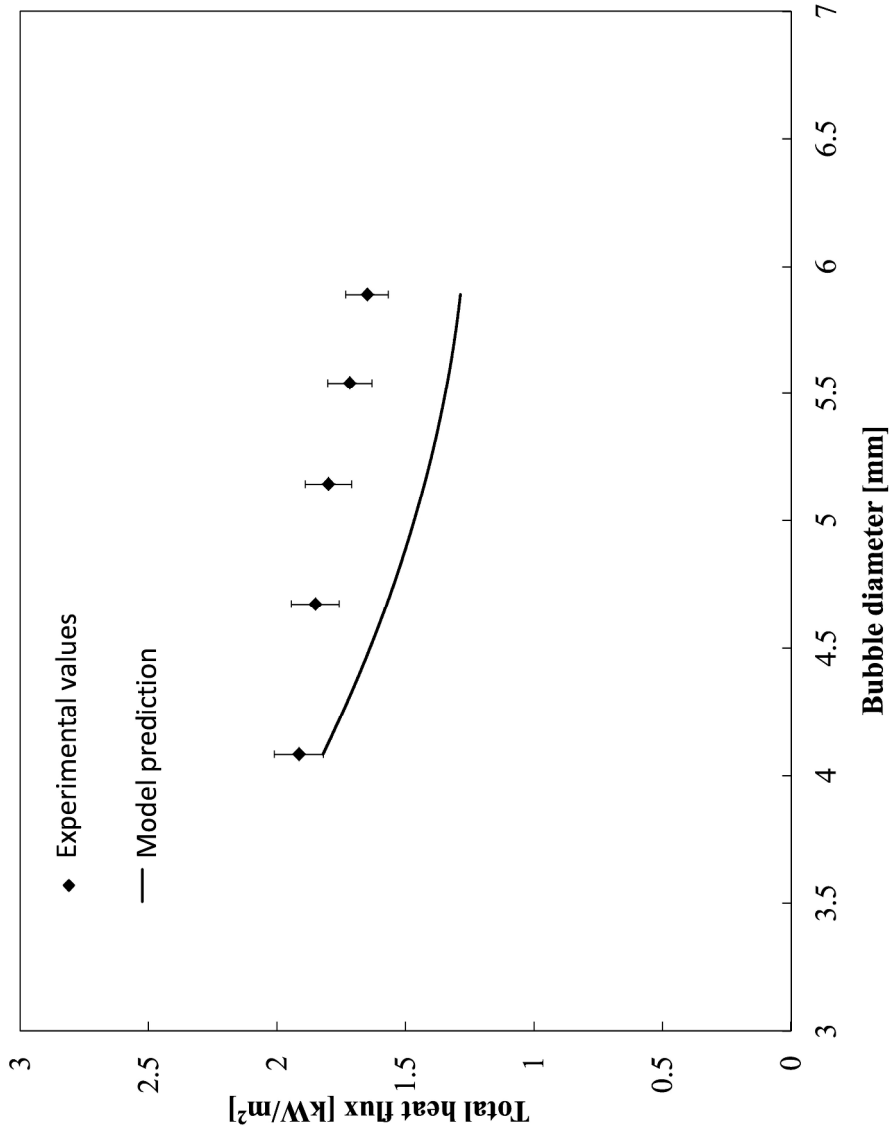

Effect of bubble diameter on the total heat flux in the bubble column measured and evaluated at $V_{g}=3.8 \hspace{2pt}\rm{cm/s};\hspace{2pt}\it{\chi_{in}} = \rm{21}\%;\hspace{2pt} \it{H}=\rm{254}\hspace{2pt}\rm{mm}$.
266x355mm (300 x 300 DPI)

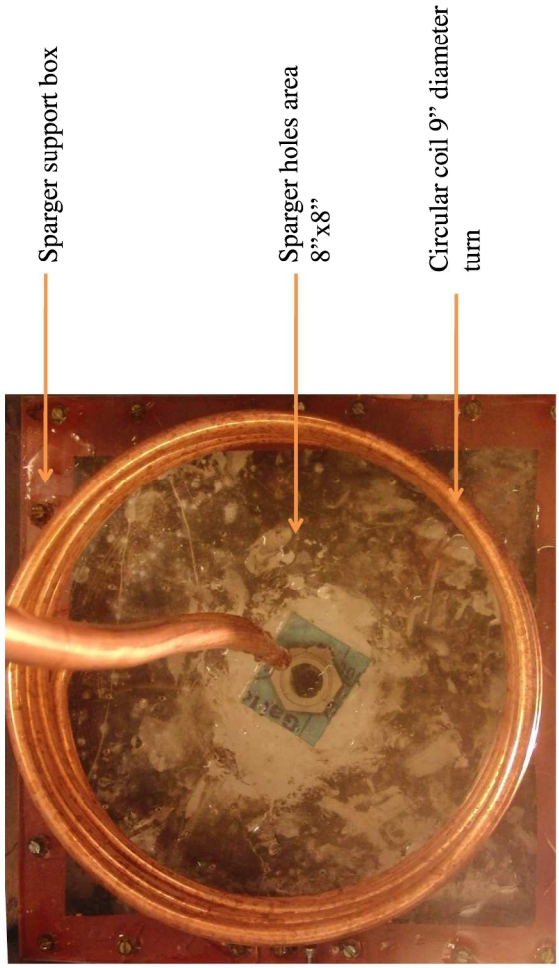

Photographs showing design of sparger and coil for (a) non-impact and (b) impact cases
254x338mm (300 x 300 DPI)